universität wien

MASTERARBEIT/MASTER'S THESIS

Titel der Masterarbeit / Title of the Master's Thesis

„Native soil organic matter composition affects the magnitude of the rhizosphere priming effect in permafrost soils“

verfasst von / submitted by

Julia Hildegard Wiesenbauer BSc

angestrebter akademischer Grad / in partial fulfilment of the requirements for the degree of

Master of Science (MSc)

Wien, 2018 / Vienna 2018

Studienkennzahl lt. Studienblatt / degree programme code as it appears on the student record sheet:	A 066 833
Studienrichtung lt. Studienblatt / degree programme as it appears on the student record sheet:	Masterstudium Ecology and Ecosystems
Betreut von / Supervisor:	Univ.-Prof. Dr. Andreas Richter

Acknowledgements

I would like to thank my thesis advisor Univ.-Prof. Dr. Andreas Richter, whose office door was always open when I had a question and always gave me good advice when I needed it.

I also want to thank Dr. Thomas Walker, who helped me a lot with the statistics and always encouraged me in my work.

Thanks to Dr. Birgit Wild and Dr. Jörg Schnecker for providing their data.

Thanks to the whole TER-division for your help and support.

Special thanks to my family and friends who provided me with unfailing support and continuous encouragement throughout my years of study and through the process of writing this thesis. This accomplishment would not have been possible without them.

Table of Contents

PART 1

General Introduction

In the period of 1880 to 2012, the globally averaged combined land and ocean surface temperature increased by approximately 0.85°C. In high latitudes, however, temperatures have risen twice as fast as on global average. Since 1875, the Arctic has warmed by 1.36°C per century and since 1979 by 0.5°C per decade (IPCC, 2013).

This warming affects soils in the northern circumpolar permafrost region that encompass an area of 17.8×10^6 km^2 (Hugelius et al., 2014).

Permafrost is defined as the ground that remains at or below 0°C for at least two consecutive years. Different permafrost zones are distinguished depending on how much of the land area is underlain by permafrost (Fig. 1). The areas where permafrost occurs everywhere beneath the exposed land surface (90-100%) is called continuous permafrost zone. The zone where some areas beneath the exposed land surface are free of permafrost while others are underlain by permafrost is called the discontinuous permafrost zone. The discontinuous permafrost zone can, based on the percentage of the land surface underlain by permafrost, be further subdivided into extensive (65-90%), intermediate (35-65%), sporadic (10-35%) and isolated patches (0-10%) of permafrost. The upper layer of the permafrost which is subjected to annual thawing and freezing is called active layer (Van Everdingen, 1998).

In the past, whenever Earth's climate became cold enough, permafrost had formed (Yershov, 1998 cited in AMAP, 2011). Around 40 million years ago, with the progressive cooling of the Earth's climate, the area occupied by permafrost started to expand. During the last glacial maximum (around 20 ky BP) more land area than today was underlain by permafrost, including significant portions of the non-glaciated territory of Europe, North America, and northern Eurasia (Fig. 2) (AMAP, 2011).

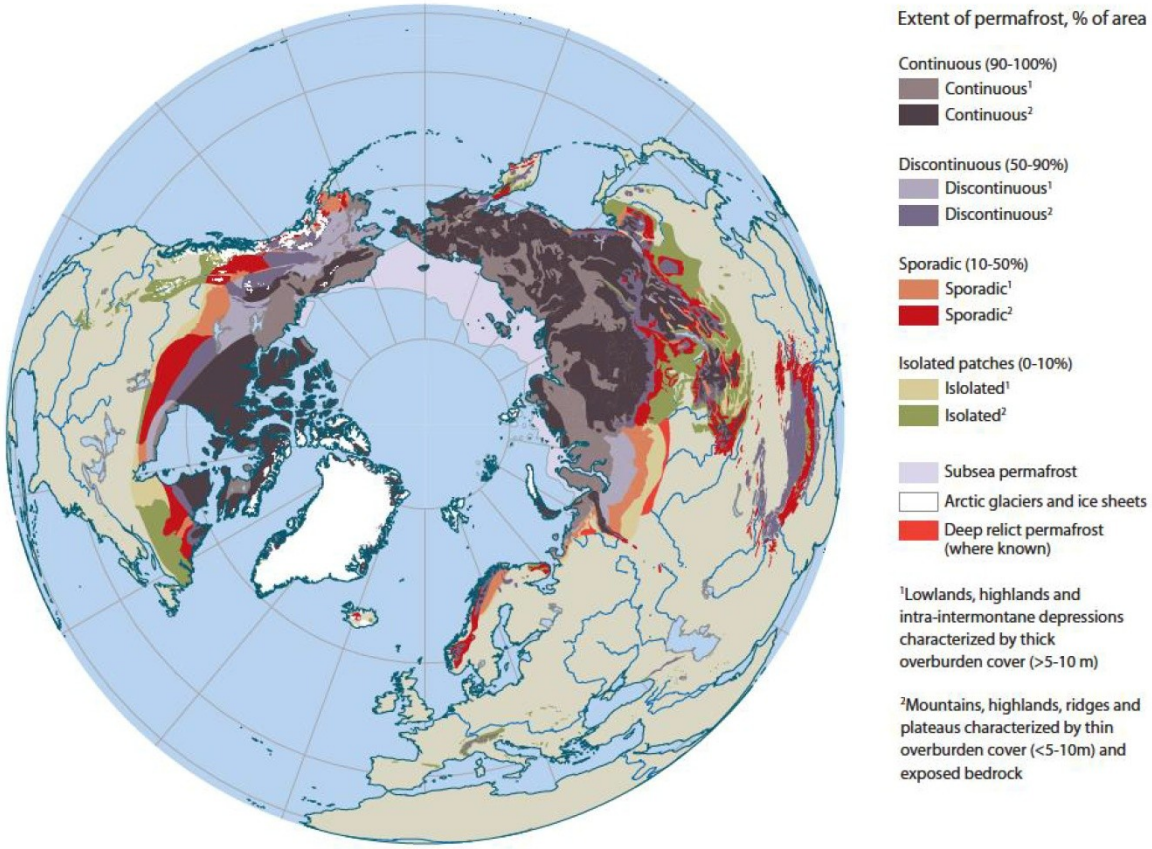

Figure 1. Extent and type of permafrost in the Northern Hemisphere. Source: International permafrost Association, Brown et al. (1998) & AMAP (2011).

The transition from the last glacial period to the current interglacial period caused permafrost to rapidly thaw from the top and from the bottom of the southernmost limits of its Late Pleistocene maximum distribution (Yershov, 1998 cited in Romanovsky et al., 2008). Typical for the early Holocene was the formation of new landscapes with many thermokarst lakes through degradation of permafrost by thermokarst processes (Schirrmeister et al., 2002). By the time of the Holocene optimum (5 to 9 ky BP) most of the deglaciated Europe, northern Kazakhstan and a significant proportion of Western Siberia in northern Eurasia were free of permafrost (Yershov, 1998 cited in Romanovsky et al., 2008) (Fig. 2). The continuous terrestrial permafrost zone, however, was generally stable with no widespread thaw. Therefore, permafrost is still present today in northern and central parts of West Siberian, in Central Siberia and in East Siberia and in the Russian Far East (Romanovsky et al., 2008).

Holocene climate was warmer and more stable than the Late Pleistocene climate; nonetheless, new shallow short-lived permafrost formed during cold

intervals, but disappeared afterwards (Romanovsky, Garagula, & Seregina, 1992; Velichko & Nechaev, 2005 cited in Romanovsky et al., 2008). The Little Ice Age around 1600 to 1850 was the last and probably coldest of these cold intervals and lead to the formation of shallow permafrost with 15 to 25 m thickness (Romanovsky et al., 1992) in sediments that had been unfrozen during most of the Holocene (Romanovsky et al., 2008). Much of today's discontinuous and sporadic permafrost was formed during this time (Grosse, Romanovsky, et al., 2011).

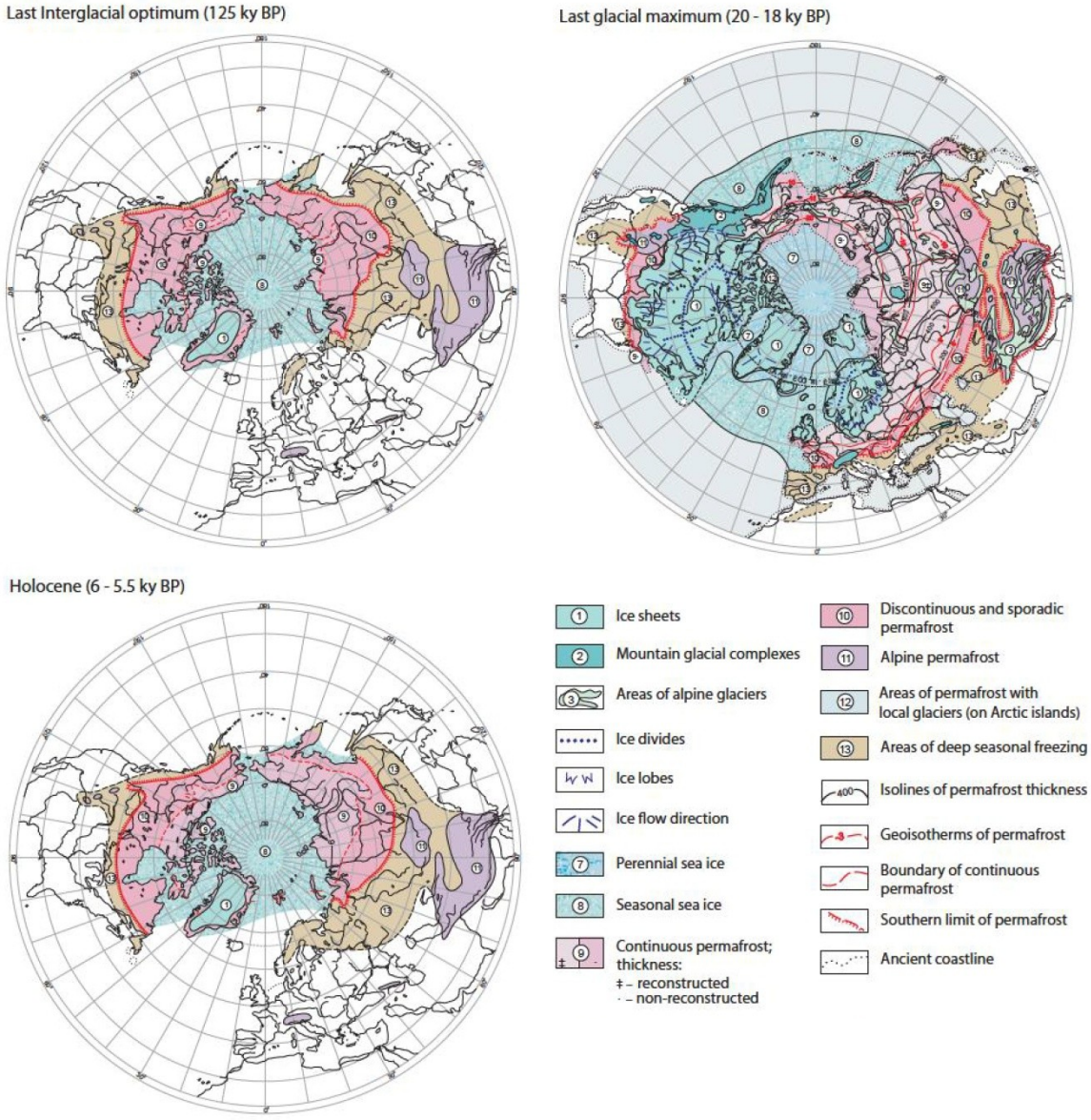

Figure 2. Permafrost distribution during the last interglacial period (125 ky BP), the last glacial maximum (20 to 18 ky BP), and during the Holocene climatic optimum (6 to 5.5 ky BP) based on

paleo-reconstructions by Velichko & Faustova (2009) and Velichko & Nechaev (2009). Source: AMAP (2011).

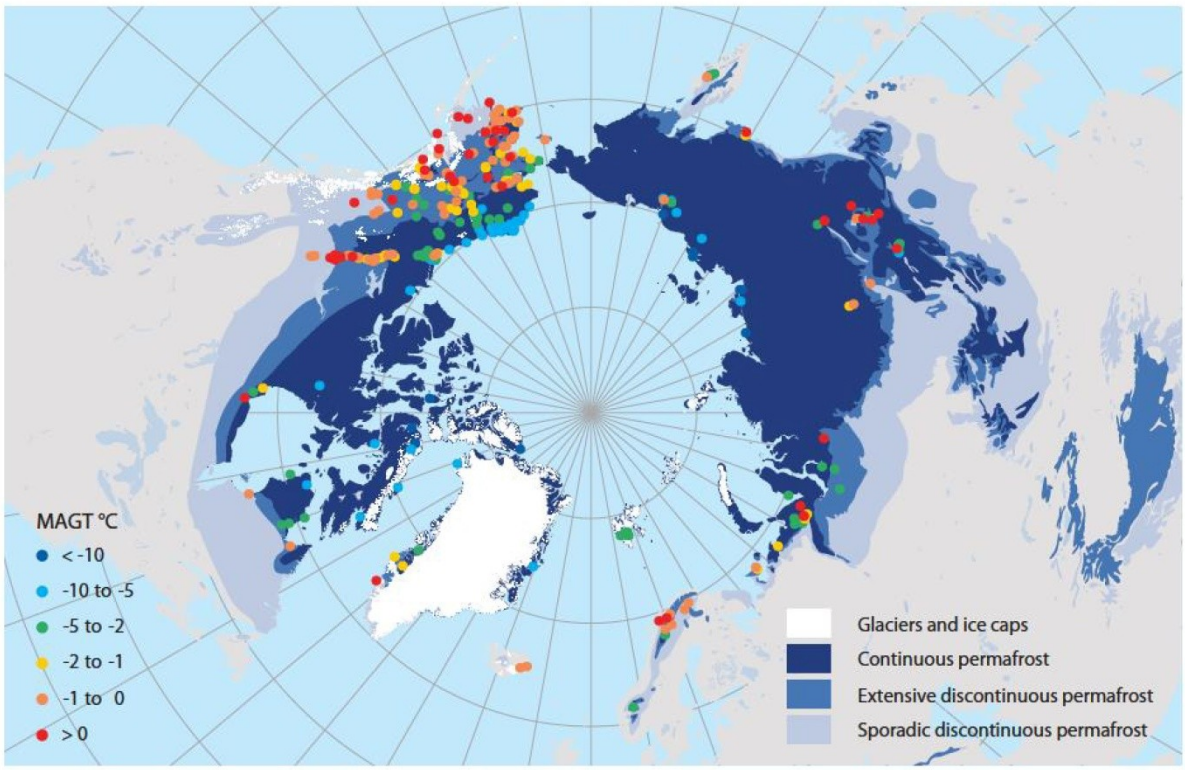

Figure 3. Mean annual ground temperature (MAGT) determined at the depth of zero annual amplitude or the nearest adjacent measurement point during the International Polar Year. Source: Romanovsky et al. (2010) & AMAP (2011).

Today's upper permafrost contains different types of deposits such as ice-rich wind-blown silt deposits ('Yedoma Ice Complex') of the late Pleistocene, fluvial and alluvial deposits, Holocene and Weichselian peat, lacustrine deposits in former thermokarst depressions and older Ice Complex deposits (Schirrmeister et al., 2011).

These permafrost soils formed syngenetically through sedimentary deposition on the soil surface. As the active layer always thaws to similar depths each summer, roots and organic matter at the bottom of the thawed soil profile were gradually incorporated into permafrost (Dutta et al., 2006; Zimov et al., 2006). The deposits vary in their total organic carbon content (TOC) that can range from about 0.1 wt% for fluvial deposits to 45 wt% in Holocene peats (Schirrmeister et al., 2011).

The accumulation of sediments, peat formation and the burial of soil organic carbon (SOC) through cryoturbation are important processes of SOC accumulation in permafrost soils (Ping et al., 1998; Schirrmeister et al., 2011). Due to the low temperatures as well as high soil-water content decomposition rates are strongly reduced in permafrost soils. This allowed old, otherwise labile carbon to persist and leads to the accumulation of massive amount of soil organic carbon (SOC) in the northern circumpolar permafrost region (Davidson & Janssens, 2006; Hugelius et al., 2013; Koven et al., 2011).

It was estimated that 1307 Pg SOC (uncertainty range of 1140-1476 Pg) are contained in the upper 3 m of soils, delta deposits and Yedoma (Fig. 4). Approximately, 999 Pg of the SOC is stored in permafrost soils of which 822 Pg are perennially frozen (Hugelius et al., 2014). Compared to the around 760 Pg carbon in the atmosphere, the amount of carbon stored in permafrost is very high (IPCC, 2013).

The Yedoma core region in Siberia and Alaska alone stores approximately 213 ± 52 Pg of SOC in the upper 3 m (Hugelius et al., 2014). The Yedoma Ice Complex is part of the continuous permafrost zone and is characterized by ice- and organic-rich loess deposits with an average depth of 25 m (10-90 m) that contain massive ice wedges that make up as much as 50% of the volume (Zimov et al., 2006).

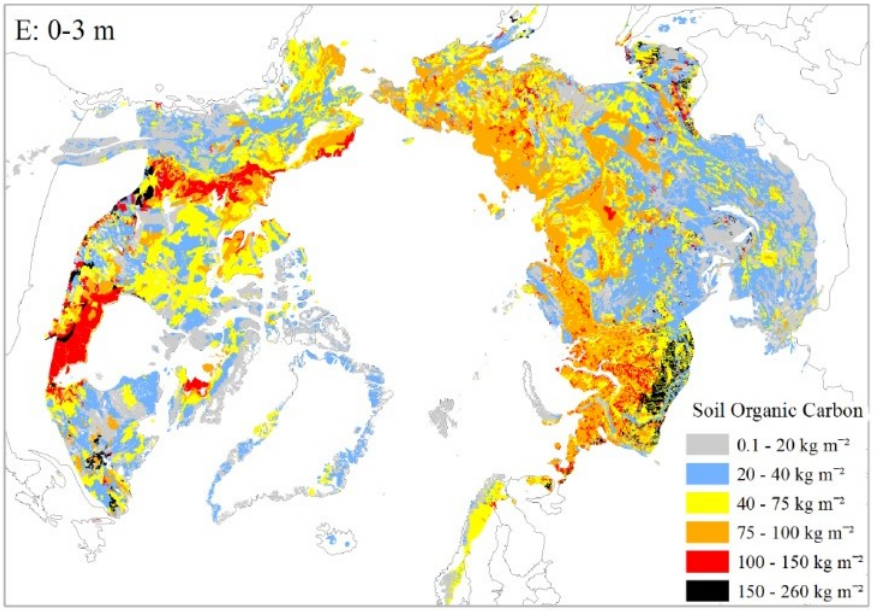

Figure 4. Map of estimated 0-3 m SOC storage (kg C m^{-2}) in the northern circumpolar permafrost region. Source: Hugelius et al. (2014)

As a response to increased air temperatures and changes in snow cover permafrost soils are now warming (Romanovsky, Drozdov, et al., 2010).

Generally, mean annual ground temperature (MAGT) at the depth of zero annual amplitude is decreasing northwards in the Northern Hemisphere (Fig. 3). In the discontinuous permafrost zone, the temperatures fall within a narrow range with MAGT at most sites being higher than -2 °C. Lower MAGT can be found in areas overlain by peat or in higher elevations. The continuous permafrost zone shows a greater range in MAGT with temperatures from more than -1 °C to less than -15 °C. Depending on the location the overall range in permafrost temperature has been decreasing by about 1 °C (Romanovsky, Smith, et al., 2010). Warming rates for warm permafrost at temperatures close to 0 °C are much smaller than for colder permafrost (< -2 °C) or bedrock (Romanovsky, Smith, et al., 2010). In the last 20 to 30 years permafrost has warmed typically by 0.5 to 2 °C at the depth of the zero annual amplitude (Romanovsky et al., 2008; Romanovsky, Smith, et al., 2010).

As a consequence, a significant fraction of permafrost is thawing, especially the permafrost formed during the Little Ice Age (Fig. 5). Recently, there are also indications that permafrost from the Late Holocene has begun to thaw in Alaska, northeastern Europe, and northwestern Siberia. Some projections even suggest that until 2100 the Late Holocene permafrost in Russia will be thawing at all locations and that even the Pleistocene permafrost might thaw (Romanovsky et al., 2008). According to estimates, current permafrost area will decrease by 53% to 66% by 2100 (Euskirchen et al., 2006; Lawrence et al., 2012; Saito et al., 2007).

If permafrost thaws, SOC that was previously protected by freezing temperatures becomes susceptible to decomposition by soil microbes (Schmidt et al., 2011). Mineralization of just a fraction of the permafrost carbon pool to carbon dioxide (CO_2) and methane (CH_4) and its release to the atmosphere could act as positive feedback to climate warming and increase the rate of climate change (Grosse, Harden, et al., 2011; Schuur et al., 2008, 2013, 2015)

Figure 5. Present-day distribution of permafrost of different ages in Russia. Source after Lisitsyna & Romanovskii (1998) & AMAP (2011).

Another process that could potentially lead to a positive-feedback on CO_2 increase and global warming by increasing soil organic matter (SOM) mineralization is the so-called 'rhizosphere priming effect' (Heimann & Reichstein, 2008). Rhizosphere priming is defined as the stimulation of the SOM mineralization by an addition of easily degradable compounds (Bingeman et al., 1953; Kuzyakov et al., 2000). These carbon (C) and nitrogen (N) containing organic compounds may originate from a steady supply of plant material, mainly rhizodeposits which include root exudates, mucilage, compounds from roots death and cells sloughed via mechanical abrasion (Jones et al., 2009).

The priming effect is thought to be the result of the alleviation of the carbon and energy limitations of the microbial community. It is believed, that soil microbes are in many cases carbon and energy limited (Schimel & Weintraub, 2003), in particular in the deep soil layers where fresh carbon inputs are very low (Fontaine et al., 2007). This low soil organic carbon (SOC) concentrations result in a physical disconnection of the microbial decomposers and their substrate (Schmidt et al., 2011). Furthermore, for the microbes to utilize the high-molecular weight compounds of the SOM they must release extracellular enzymes to degrade them into smaller molecules that can be assimilated. However, the synthesis of extracellular enzymes is energy-costly and enzymes also contain C

(Schimel & Weintraub, 2003). Consequently, the net energy gained by the degradation of complex recalcitrant SOM compounds is too little to sustain high microbial activities, particularly in deeper soil horizons where C concentrations are low and more enzymes need to be produced to degrade an unit of C (Don et al., 2013; Fontaine et al., 2007). Hence, it was suggested that the percentage of dormant or inactive cells increases with soil depth (De Nobili et al., 2001; Spohn et al., 2016). As a result, SOM decomposition is strongly reduced due to carbon and energy limitations of the microbial decomposers, especially in deep soils where carbon concentrations are low (Fontaine et al., 2007; Rumpel & Kögel-Knabner, 2011; Schmidt et al., 2011). These constraints may be alleviated by an increased availability of easily assimilable organic compounds, stimulating SOM decomposition in subsoils (Wild et al., 2014, 2015, 2016). The input of easily available carbon may activate dormant microorganisms ('triggering effect') (De Nobili et al., 2001; Fontaine et al., 2007) and provides them with the necessary energy to produce extracellular enzymes capable of degrading complex SOM (E. Blagodatskaya & Kuzyakov, 2008; Dijkstra et al., 2013; Fontaine et al., 2003, 2007; Kuzyakov, 2010). This increase in SOM decomposition caused by an input of labile organic compounds is referred to as 'positive priming effect' (Kuzyakov et al., 2000).

However, the input of easily available organic compounds can also decrease SOM decomposition which is called 'negative priming effect' (Kuzyakov et al., 2000). Negative priming occurs when the microorganisms utilize the added labile substrate instead of decomposing the recalcitrant native SOM to meet their carbon and energy requirements ('preferential substrate utilization') (E. V Blagodatskaya et al., 2007; Dijkstra et al., 2013; Guenet et al., 2010; Kuzyakov et al., 2000). Negative priming effects are not described as often as positive priming effects. Nonetheless, negative priming effects could be of great importance for ecosystems by replacing losses of the SOM (Kuzyakov et al., 2000).

Another explanation for the priming effect is the 'nitrogen mining hypothesis' (Craine et al., 2007; Dijkstra et al., 2013; Fontaine et al., 2011). It has been proposed that the microbial growth may be stimulated by the additional carbon causing a higher microbial N demand. To meet their nutrient requirements, microbes may decompose SOM to release N, which is referred to as 'nutrient mining' (Craine et al., 2007; Dijkstra et al., 2013; Fontaine et al.,

2011). In addition, the nitrogen in the degradable organic matter further promotes the synthesis of extracellular enzymes capable of degrading polymeric compounds of the SOM (Allison et al., 2009).

Further, the input of fresh organic matter is also thought to initiate a succession of microbial groups. First, fast-growing microorganisms ('r-strategists') that metabolize most of the easily assimilable organic matter are stimulated. Their subsequent death leads to a release of microbial biomass-derived CO_2, sometimes referred to as 'apparent priming effect' (Kuzyakov, 2010). Opposed to real priming, where there is an increase in the decomposition of SOM, the apparent priming effect is caused by an increase of microbial C turnover, which is not linked to changes of SOM decomposition (Jenkinson et al., 1985). The microorganisms mainly responsible for the real priming effect are slow growing bacteria and fungi ('K-strategists') that preferentially degrade complex carbon compounds (Fontaine et al., 2003). They profit from the bacterial necromass remaining after the easily available compounds are exhausted and r-strategist turnover has increased. They produce a surplus of extracellular enzymes that results in a co-metabolic decomposition of SOM and thus leads to the 'real priming effect' (E. Blagodatskaya et al., 2014; Fontaine et al., 2003).

Overall, there is an agreement that the soil microbial biomass plays a key role in the processes leading to the real priming effect (Fontaine et al., 2003; Kuzyakov et al., 2000). Nevertheless, there are still many ambiguities regarding mechanisms and controls of the priming effect (Heimann & Reichstein, 2008; Kuzyakov et al., 2000; Zhu et al., 2014). Generally, it is becoming recognized that the rhizosphere priming effects on SOC decomposition can play important roles in the global carbon cycle (Cheng et al., 2014; Heimann & Reichstein, 2008; Kuzyakov, 2010). However, the magnitude of the impact of the priming effect on SOM decomposition in general, and particularly in high-latitude soils in a future warmer climate is for the most part uncertain.

Nonetheless, there are indications that in the future the magnitude of the priming effects and the associated carbon losses from arctic permafrost soils may increase (Wild et al., 2016).

As a consequence of the rising temperatures plant productivity in the Arctic is increasing, which is known as 'tundra greening' (Bhatt et al., 2010; Grosse et

al., 2016; Hicks Pries et al., 2016; Natali et al., 2012). Monitoring of the Arctic tundra vegetation by Earth-Observing Satellites (EOS) that takes place since 1982 confirms that there is a trend towards increased yearly maximum above-ground vegetation and total aboveground vegetation productivity (Richter-Menge et al., 2017). This increase in plant productivity further implies an increased transport of organic compounds belowground (Wild et al., 2016). In addition, several studies have suggested that under elevated CO_2 rhizodeposition will increase (Darrah, 1996; Pendall et al., 2004; Fransson and Johansson, 2010), which could further increase priming.

Moreover, in many areas, the active layer thickness increased by a few to tens of centimeters since the 1990s (IPCC, 2013). Usually, the rooting depth in tundra soils is rather shallow (Jackson et al., 1996), and active carbon cycling concerns only the 20 uppermost centimeters near the surface (Khvorostyanov et al., 2008). However, an increasing active layer thickness may promote an increase in the intensive deep rooted zone and induce the loss of deep carbon (Heimann & Reichstein, 2008).

The increased availability of labile plant-derived compounds could potentially increase rhizosphere priming effects and result in the release of additional carbon to the atmosphere if photosynthetic uptake is not increased as well (Hartley et al., 2012). It has been shown that exudation of carbon compounds by living roots can suppress 50% or stimulate up to 400% of SOM decomposition (Zhu et al., 2014). Due to the potential impact, the rhizosphere priming effect might have on SOM mineralization and climate, it is important to better understand the controls governing the priming effect.

It has been suggested that the amount of microbial biomass and the microbial community structure affect SOM mineralization when labile carbon is added (E. Blagodatskaya & Kuzyakov, 2008; Garcia-Pausas & Paterson, 2011), caused by different microbial taxa that are involved in the decomposition of different SOM fractions (Fontaine et al., 2003, 2011). Additionally, the added substrate also exerts substantial control over the priming effect. It was found that the amount of the carbon-containing substrate added influenced the direction and the magnitude of the priming effect (E. Blagodatskaya & Kuzyakov, 2008; Guenet et al., 2010). If the added carbon was up to 15% of microbial biomass carbon

pool, an increased SOM decomposition took place, i.e., positive priming effect (E. Blagodatskaya & Kuzyakov, 2008). However, much higher amounts of added carbon could result in a preferential substrate utilization and a 'negative priming effect', i.e. reduced SOM decomposition (E. Blagodatskaya & Kuzyakov, 2008; Dijkstra et al., 2013; Guenet et al., 2010; Kuzyakov et al., 2000).

Other studies observed that in addition to the amount, the quality of the added substrate played an important role in determining the priming effect (Di Lonardo et al., 2017; Jagadamma et al., 2014; Wild et al., 2014, 2016). Di Lonardo et al. (2017) showed that the priming effect was much more dependent on the substrate structure rather than the energy that the added substrate provided for microbial use. Compounds that were energy-poor but resembled the recalcitrant SOM triggered a stronger priming effect than simple energy-rich compounds (Di Lonardo et al., 2017). This is in line with the mechanisms proposed by Van der Wal & De Boer (2017). They propose that in order for a positive priming effect to occur there must be an overlap in the chemical properties of the added substrate and the native SOM as well as the functional potential of the microbial community, which then determines the extent of the priming effect (Van der Wal & De Boer, 2017).

This suggests that the priming effect is not only the result of a relationship between the microbial community structure and the added substrates. The composition of SOM potentially also plays a crucial role in determining the extent of the priming effect. It has already been shown in several studies that the SOM degradation was affected by its composition (Drake et al., 2015; Hernández & Hobbie, 2010; Jagadamma et al., 2014; Paré & Bedard-Haughn, 2013; Yang et al., 2016). SOM composition may also help to explain how the addition of the same or similar carbon compounds to different soils could trigger different priming effects (Hamer & Marschner, 2005). The same might apply to the different extent of priming effect that was observed among different ecosystems by labile carbon compounds (Liu et al., 2017). Furthermore, differences in the priming effect were also found for different soil horizons in permafrost soils (Wild et al., 2016). Previously, differences in priming effect had been associated with different carbon-to-nitrogen (C/N) ratios of the SOM and the resulting limitations for the microbial community (Vance et al., 2001; Wild et al., 2014, 2016). However, there may also be certain fractions of the SOM which in response to

substrate addition are more strongly decomposed, i.e., are more prone to priming than other SOM fractions. It is also possible that specific microbial groups could be stimulated by the substrate addition and subsequently decompose certain SOM fractions.

There might be a relationship between the microbially mediated rhizosphere priming effect and the SOM composition, but further investigations are needed to elucidate this relationship.

PART 2

MANUSCRIPT

„Native soil organic matter composition affects the magnitude of the rhizosphere priming effect in permafrost soils“

Introduction

Temperatures are rising twice as fast at higher latitudes than the global average (IPCC, 2014). As a result of this warming, plant productivity in Arctic regions is increasing (Bhatt et al., 2010; Grosse et al., 2016; Hicks Pries et al., 2016; Natali et al., 2012). Additionally, warming may increase active layer thickness of permafrost soils (AMAP, 2011), which may promote more intense rooting and enable plant roots to penetrate deeper soil layers that were not previously rooted (Heimann & Reichstein, 2008). Together with the rise in plant productivity, this implies an increased belowground carbon allocation (Wild et al., 2016), primarily by rhizodeposition (root exudates, root litter, slough-off cells, mucilage) (Jones et al., 2009).

The additional plant-derived carbon in soil, however, may not necessarily lead to an increased soil carbon stock as observed in some studies (e.g. Sistla et al., 2013). On the contrary, the input of easily degradable compounds may also stimulate the soil organic matter (SOM) mineralization by a process called 'rhizosphere priming effect' (Bingeman et al., 1953; Kuzyakov et al., 2000), which may result in the release of carbon to the atmosphere (Hartley et al., 2012). Permafrost soils at higher latitudes, contain an estimated stock of about 1035 Pg of soil organic carbon (SOC) in the upper 3 m, of which 822 Pg are currently perennially frozen (Hugelius et al., 2014). Mineralization of just a fraction of the soil organic matter (SOM) stored in permafrost soils could lead to a significant increase of carbon dioxide (CO_2) and methane (CH_4) concentrations in the atmosphere thereby inducing a positive feedback to climate warming (Grosse, Harden, et al., 2011; Schuur et al., 2008, 2013, 2015).

So far, there are several hypotheses on the mechanisms by which the priming effect is caused. First, the priming effect is thought to be the result of alleviating the carbon (C) and energy limitation of microbial communities that arises from low accessibility of organic C due to low concentrations (physical disconnection) or associations of organic matter with minerals (Schmidt et al., 2011). The input of easily assimilable organic compounds by plant roots provides microbes with the necessary energy to start growing and synthesize extracellular enzymes for the degradation of SOM (E. Blagodatskaya & Kuzyakov, 2008; Dijkstra et al., 2013; Fontaine et al., 2003, 2007; Kuzyakov, 2010). Consequently,

increased availability of easily assimilable carbon can strongly stimulate SOM decomposition (Wild et al., 2014, 2015, 2016), particularly in arctic subsoils where fresh carbon inputs and carbon concentrations are very low (Rumpel & Kögel-Knabner, 2011).

Second, the additional carbon can also stimulate net growth of microbes (i.e. an increase in microbial biomass) leading to an increased microbial nitrogen (N) demand which results in nitrogen mining, i.e., the degradation of SOM to meet the nitrogen demand of the microbial community (Craine et al., 2007; Dijkstra et al., 2013; Fontaine et al., 2011).

Third, the priming effect may also be explained by a succession of functional groups of microbes. It is thought, that initially, easily assimilable plant inputs stimulate growth and turnover of fast-growing microorganisms ('r-strategists'), which leads to a release of CO_2 from their increased biomass turnover, known as 'apparent priming effect' (Kuzyakov, 2010). After the easily assimilable substrates are exhausted, fast-growing microbes are replaced by slow-growing bacteria and fungi ('K-strategists') that benefit from the emerging necromass of r-strategists. The K-strategists then start to degrade more recalcitrant carbon (Fontaine et al., 2003), which is also called co-metabolic decomposition of SOM and is thus a 'real priming effect' (E. Blagodatskaya et al., 2014; E. Blagodatskaya & Kuzyakov, 2008; Fontaine et al., 2003).

Generally, it is increasingly recognized that the effect of rhizosphere priming on SOM decomposition may play an important role in the global carbon cycle (Cheng et al., 2014; Heimann & Reichstein, 2008; Kuzyakov, 2010). However, the magnitude of the impact of the priming effect on SOM decomposition in general, and specifically in high-latitude soils in a future climate is still for the most part uncertain. Besides, there are still many ambiguities regarding mechanisms and controls of the priming effect, that hamper our capabilities to predict changes in priming effect with changing environmental conditions (Heimann & Reichstein, 2008; Kuzyakov et al., 2000; Zhu et al., 2014).

There is a general understanding that the soil microbial activity plays a key role in the controlling the rhizosphere priming effect (Fontaine et al., 2003; Kuzyakov et al., 2000). Additionally, it has been suggested that the microbial community structure and the amount of microbial biomass influence SOM mineralization (E. Blagodatskaya & Kuzyakov, 2008; Garcia-Pausas & Paterson,

2011). Furthermore, the amount of the added carbon-containing substrate affected the direction and the magnitude of the priming effect (E. Blagodatskaya & Kuzyakov, 2008; Guenet et al., 2010) as did the substrate quality (Di Lonardo et al., 2017; Jagadamma et al., 2014; Wild et al., 2014, 2016).

In addition to the microbial community structure and activity and the added substrate quantity and quality, the composition of soil organic matter may potentially also be crucial in determining the magnitude of the priming effect. Although it has already been shown in several studies that the SOM degradation was affected by its composition (Drake et al., 2015; Hernández & Hobbie, 2010; Jagadamma et al., 2014; Paré & Bedard-Haughn, 2013; Yang et al., 2016), little is known about the effect of the SOM composition on the priming effect. Differences in the SOM composition may for example explain how the addition of the same carbon compounds to different soils resulted in different priming effects (Hamer & Marschner, 2005). This might also apply to the differences in the priming effect that were observed for different soil horizons in permafrost soils (Wild et al., 2016). There could be specific compounds or groups of compounds of the SOM, for which decomposition additional substrates are necessary, i.e., which are more prone to priming. It is also possible that specific microbial groups could be stimulated by the substrate addition and subsequently decompose certain SOM fractions, which would imply that an interaction of the microbial community composition and soil organic matter composition exists for the priming effect. Therefore, studies investigating possible relationships between the microbial-mediated priming effect and the SOM composition, are urgently needed.

The overall aim of this study was to determine if the rhizosphere priming effect is affected by the composition of SOM. Specifically, we wanted to elucidate whether certain classes of substances were affecting priming more than others.
Expecting that SOM quality plays an important role for heterotrophic respiration and rhizosphere priming, we hypothesized, (1) that complex organic matter (i.e. OM that requires more enzymatic steps to be broken down) will result in lower respiration rates than SOM with a higher proportion of easily assimilable compounds. Additionally, we hypothesized (2) that the priming effect would be higher in soil where soil organic matter consisted to a greater extent of complex compounds and compounds which breakdown products may be potentially toxic

to microbes (e.g., aromatics and phenols), compared to soils containing higher proportions of easily degradable compounds (e.g., plant-derived carbohydrates). Because the production of extracellular enzymes which are ultimately responsible for a priming effect requires carbon and nitrogen, we tested whether the addition of carbon (cellulose) alone or carbon in combination with nitrogen (protein) would differentially affect the relationship between soil organic matter and priming.

We analyzed a total of 106 samples derived from five soil horizons of four sites across the Siberian Arctic. The SOM composition was determined by pyrolysis-gas chromatography mass spectrometry (Py-GC/MS) measurements. Data on respiration and priming effects were obtained from a previous study in which identical soil samples were incubated under similar conditions with (priming effect) or without (respiration) addition of substrate (Wild et al., 2016). Soils were incubated with cellulose or with protein to account for potential differences in the priming effects between the addition of either an organic carbon or organic nitrogen source. We explored the relationship of SOM composition with both the respiration and the priming effect by standardized linear mixed effects models.

Material and Methods

Soil sampling

In the course of the CryoCARB project (http://www.univie.ac.at/cryocarb/the-cryocarb-project/), soils were sampled at four sites in the Siberian Arctic along a west-east transect in the areas Tazovskiy, Ari-Mas, Logata, and Cherskiy. At each site, six pits were dug down to the permafrost table and a total of 106 soil samples were taken from five soil horizons. The number of samples taken per pit and per horizon varied and per pit not always all 5 horizons were sampled. We sampled soil from the active layer and permafrost. In the active layer, we sampled the organic topsoil, the mineral topsoil, the mineral subsoil and cryoturbated material. The cryoturbated material, which originates from the burial of topsoil through repeated thawing-freezing cycles (Bockheim, 2007), was sampled at a similar depth to the mineral subsoil. The upper 15 cm of the permafrost were sampled.

Living roots were removed directly after sampling and soils were air-dried and stored under dark, cool and dry conditions. For a more detailed description of sites and sampling refer to Gentsch et al. (2015) and Wild et al. (2016).

Pyrolysis - gas chromatography/ mass spectrometry

We determined the chemical composition of the soil organic matter (SOM) using pyrolysis-gas chromatography/ mass spectrometry (Py-GC/MS) on all samples.

Before Py-GC/MS aliquots of the air-dried soil samples were finely ground. Approximately 0.5-1 mg of soil were pyrolyzed (Pyroprobe 5250, CDS Analytical) by first holding the temperature at 50 °C for 5 s and then increasing the temperature by 20 °C/s until 600 °C, at which point the temperature was held for 20 s. Helium was used as a carrier gas at a flow rate of 1 ml/min. The samples were carried onto a 0.25 mm x 30 m column (Supelco SUPELCOWAX® 10) in a gas chromatograph (Trace GC ULTRA, Thermo Scientific). The column temperature was held at 50 °C for 2 min to trap and focus the volatile compounds, then heated up to a final temperature of 270 °C at a rate of 7 °C/min and held for 5 min, resulting in a total run time of 38 min. Eluting compounds were detected with a mass spectrometer (ISQ, Thermo Scientific) and total ion

chromatograms (TICS) were reconstructed. The injector temperature was set to 280 °C and the transfer line and ion source temperatures were set to 270 °C. The compounds of interest eluted between 7 and 28 min.

Py-GC/MS data were processed with Chromeleon 7.2 SR4. Chromatogram peak areas were integrated with the Cobra algorithm with manual changes where necessary. Compounds were identified based on their mass spectra with the NIST Mass Spectral Search Program 2.2.

Identified compounds were subsequently assigned to chemical classes from which they most likely derived from based on their chemical structure.

Priming experiment - cumulative respiration and response ratios of soils amended with cellulose or protein

In this study, we used data on SOC mineralization from a study by Wild et al. (2016), that was carried out on identical samples. Wild et al. (2016) had investigated the priming effect in Siberian soils in an incubation experiment in which they added cellulose or protein to the soil as a proxy for root exudates.

From this study, we used the cumulative respiration (µmol C g^{-1} DW) which is the sum of CO_2 derived from SOC mineralization after 25 weeks of incubation of untreated soils. Further, we used the so-called response ratios (cellulose response, protein response) which were obtained as a ratio of the CO_2 derived from SOC mineralization of cellulose or protein amended soils over CO_2 derived from SOC mineralization in untreated soil. Thus, response ratios represent the priming by cellulose or protein addition. Here, we refer to response ratios as cellulose priming and protein priming. For instance, a cellulose priming of two indicates that mineralization of SOC doubled as a consequence of cellulose addition whereas a cellulose priming of one indicates that there was no change in mineralization after cellulose addition.

Statistical analysis

All statistical analyses were performed with R 3.1.3 (R Development Core Team, 2015).

We performed a principal component analysis (PCA) with the *pca* function from the *mixOmics* package (Le Cao et al., 2015) to reduce our Py-GC/MS data into

fewer principal component axes that we used as explanatory variables in our models.

All explanatory variables and response variables that we intended to use in our models were mean centered and divided by twice the standard deviation using the *rescale* function from the *arm* package (Gelman & Su, 2015) to guarantee the same unit variance. Subsequently, standardized linear mixed effects models (standardized LMEs) were generated with the *lme* function from the *nlme* package (Pinheiro et al., 2015).

To determine whether sites or horizons differed in the relative amount of chemical compound classes or SOM composition we carried out ANOVAs, Welch's t-test or Kruskal-Wallis tests.

Graphs were created with the package *ggplot2* (Wickham, 2009).

Principal component analysis

We are aware that factor analysis has often been used in studies investigating Py-GC/MS measurements (Buurman et al., 2005; Schellekens et al., 2009; Vancampenhout et al., 2009; Yassir & Buurman, 2012). Factor analysis is well-suited to investigate the relationship of variables as its factors maximize the covariance of the variables (the common variability). However, since PCA maximizes the explained total variance it is more suited for using the resulting principal component axes as explanatory variables in a model. Furthermore, PCA components are always uncorrelated in contrast to the axes of the factor analysis, which could have been a problem in the building of a mixed effects model. Therefore, we performed a PCA to reduce our 151-dimensional Py-GC/MS data into a series of linear axes that incorporate the maximum amount of variance in the data.

Prior to this, we converted the peak areas of each sample into relative areas (%) stated as percentage of the sum of all integrated peaks of the respective sample. Moreover, we had to consider that Py-GC/MS measurements produce censored data. This implies that the absence of a compound in a chromatogram can imply two things: either the compound is not present in the sample, or it is present in concentrations too low to be detected. To overcome the possible bias that we would have generated by replacing the undetected values with zeros we decided

to instead rank our data for each compound separately (Helsel, 2012). Within each compound, all values below the detection limit were assigned the same average rank, which was below the rank of the detected compounds. Furthermore, to guarantee the same unit variance, all variables were normalized by mean subtraction and division by the standard deviation preceding PCA.

The scores and loadings of the first three principal component axes were extracted for further use.

Standardized Linear Mixed Effects Models

We performed three separate models to explain differences in *cumulative respiration* (n = 106), *cellulose priming* (n = 101) and *protein priming* (n = 106) caused by SOM composition.

We started with an initial model in which the first three principal component axes (*PC1*, *PC2*, *PC3*), representing SOM composition, were used as explanatory variables. To account for possible differences between horizons in regards to the effect of the explanatory variables (*PC1*, *PC2*, *PC3*) on the response variable, we included two-way interaction terms between each PC and *horizon*. *Horizon* was considered as a factor with five levels: organic topsoil, mineral topsoil, mineral subsoil, cryoturbated material and permafrost soil. The fixed effect structure of our initial models was:

response variable ~ PC1 + horizon + PC2 + PC3 + PC1:horizon +

PC2:horizon + PC3:horizon

Furthermore, we expected that samples originating from the same site and pit were more alike in their soil organic matter composition than they were to other samples. This relatedness would not be taken into consideration by a linear regression model, which would be a violation of the independence assumption. As such, we performed standardized linear mixed effects models (LME) with *site* and *pit* as nested random effects.

Random effects: ~ 1 | site / pit

Where necessary, we further accommodated for the different variances between horizons by weighting the *horizon* variable. The introduction of this constant variance function allowed for different constant variances for each

horizon. Each level of the *horizon* factor (except for one *horizon* level that was taken as reference) received a coefficient that represented the ratio between the variance of the *horizon* level and the variance of the reference. The introduction of the *horizon* as variance covariate significantly ($p<0.05$) improved all three models (Tab. 1) and got rid of the remaining heteroscedasticity in the residuals.

Variance structure: ~ 1 | horizon

Tab. 1. Result table of likelihood ratio test comparing standardized linear mixed effects models including and excluding *horizon* as variance covariate.

response variable	variance covariate	Df	AIC	BIC	logLik	L Ratio	p-value
respiration	*horizon*	27	-327.12	-255.21	190.56		
		23	32.60	93.86	6.70	367.72	<0.001
cellulose priming	*horizon*	27	160.34	230.68	-53.17		
		23	168.25	228.17	-61.12	15.91	<0.01
protein priming	*horizon*	27	68.25	139.91	-7.13		
		23	76.07	137.12	-15.04	15.82	<0.01

df degree of freedom, *AIC* Akaike information criterion, *BIC* Bayesian information criterion
logLik log likelihood, *L Ratio* likelihood ratio

Standardized LME models were fitted by maximum likelihood.
We assumed a Gaussian distribution and examined the model residuals for normal distribution to confirm goodness of fit. Further, we plotted the residuals against each explanatory variable to confirm homoscedasticity.

In the standardized LME model predicting the protein priming, we had to exclude one sample with an anomalously high value for protein priming because of its strong influence on the resulting model.

The significance of each parameter in explaining the variation of the response variable was tested by likelihood ratio test (LRT). To obtain the final best-fit standardized LME models we based our variable selection on p-value based stepwise deletion of the least significant ($p<0.05$) fixed effects.

Analysis of variance

Differences in the proportion of chemical compound classes between sites and horizons were tested with either an analysis of variance (ANOVA), a Welch's t-test for unequal variances or a Kruskal-Wallis test.

Separation of sites, horizons and chemical compound classes along the first three principal component axes was tested with either an ANOVA followed by the Tukey's test for post hoc comparisons or with Welch's t-test with subsequent pairwise t-test with Bonferroni correction or a Kruskal-Wallis test with subsequent Nemenyi test.

Result

Pyrolysis - gas chromatography/ mass spectrometry

Soil samples had been taken from six different soil horizons (organic topsoil, mineral topsoil, mineral subsoil, cryoturbated material, permafrost soil) at four sites (Tazovskiy, Ari-Mas, Logata, Cherskiy) in the Siberian Arctic along a west-east transect. In order to characterize their soil organic matter (SOM) composition, soil samples (n=106) originating from different sites and horizons were analyzed by pyrolysis - gas chromatography/ mass spectrometry (Py-GC/MS).

By pyrolysis, larger SOM constituents are thermally degraded into smaller molecules ('pyrolysates') which can be separated and analyzed by gas chromatography-mass spectrometry (GC/MS) (Ma et al., 2014; Vancampenhout et al., 2009). The advantage of the pyrolysis is, that the fraction of the SOM which is normally non-volatile at 300 °C, can be analyzed by breaking up the large molecules (White et al., 2004). It should be noted, that the peaks found in the chromatogram are pyrolysates of the original SOM compounds in which they normally cannot be found. Furthermore, it is likely that one compound breaks up into several pyrolysates which in turn can be derived from several different SOM compounds. Therefore, one should consider Py-GC/MS results to be a "fingerprint" of the SOM composition of the measured sample (White et al., 2004). However, most pyrolysates can be assigned to the chemical class from which they are derived.

We found a total of 151 pyrolysates in our samples from which we could identify 111 based on their mass spectra. We were not able to identify the remaining 40 pyrolysates with a sufficient certainty with the NIST Mass Spectral Search Program 2.2 library. Nevertheless, the unidentified compounds were included in the principal component analysis, where they are displayed as "unknown" in the plots.

All 111 identified pyrolysates and their assigned chemical compound class are listed in Table S1. Eighty-eight of the identified pyrolysates could be assigned to chemical classes because their origin was reported in previous studies (Buurman et al., 2005; Carr et al., 2010; Ninnes et al., 2017; Stewart, 2012;

Vancampenhout et al., 2009). The remaining 23 identified pyrolysates were assigned to chemical compound classes based on similarities in their chemical structure to the already assigned pyrolysates and are marked by a *-symbol in Table S1.

We distinguished 6 chemical compound classes: aromatics, carbohydrates, lipids, lignin derivatives, nitrogen-containing compounds, and phenols. The aromatic class is dominated by benzene- and indene-related structures and also includes styrene and three polyaromatic compounds. Carbohydrates encompass a range of polysaccharide derivatives, including furans, furaldehydes, 2-cyclopenten-1-ones, furanones and monomeric sugars. Lipid-derived compounds include alkanes and alkenes with carbon chains of 12-19 C and 12-21 C length, respectively. Lignin derivatives are made up of guaiacols, syringol, and two non-specific lignin-derived compounds. The nitrogen-containing compounds are comprised of pyrroles, indoles, and pyridines, while the phenol compound class is primarily made up of methylated phenols.

Native soil organic matter composition

Figure 1 provides an overview of the soil organic matter (SOM) composition and the average percentage share to which the SOM consists of each chemical compound class.

The SOM composition of the geographically close Central Siberian sites Ari-Mas and Logata was quite similar in terms of the chemical compound classes it is comprised of (Fig. 1 A). In contrast to Tazovskiy (West Siberia) and Cherskiy (East Siberia), the SOM in Ari-Mas and Logata consists to a larger extent of aromatic compounds and to a lower extent of carbohydrates. Although we found significant differences of the mean percentage of most compound classes between sites, the SOM composition was overall quite similar with the exception of carbohydrates and aromatics (Fig. 1 A, Tab. 2).

However, the differences in SOM composition between soil horizons was more pronounced. We observed a decrease in the proportion of carbon-containing compounds (carbohydrates, lignins) with simultaneous increase in the proportion of the nitrogen-containing compounds with depth (Fig. 1 B, Tab. 2),

suggesting a decreasing C/N ratio and presumably also a decline in the carbon content with an increase in the nitrogen content.

Furthermore, we observed an increase of aromatic compounds with depth (Tab. 2). Remarkable were the high contents of aromatic compounds in the mineral subsoil, which were mainly due to the soil samples from the Central Siberian sites, Ari-Mas and Logata (Fig. 2). The SOM in the permafrost soil was largely composed of nitrogen-containing compounds and, to a lesser extent than in all the other horizons, of carbohydrates. In contrast, the organic topsoil was not only comprised of high relative amounts of carbohydrates but also of by far the largest proportions of lignin-derived compounds, indicating an input of fresh plant material. Mineral topsoil and cryoturbated material were very similar in their SOM composition.

Interestingly, although the share of unknown compounds (i.e. unidentifiable pyrolysis products) did not differ between sites, it declined with soil depth (Fig. 1 A & B, Tab. 2). These unknown compounds could be the pyrolysis products of complex plant material, which decreased with depth, same as the plant influence.

Tab. 2. Summary table of variance analyses illustrating the significant differences ($p<0.05$) in the proportion of the compound classes between sites or horizon.

	compound class	test statistic	p-value	Test
Site	Aromatic	$X^2(3) = 22.14$	<0.001	Kruskal-Wallis
	Carbohydrate	$X^2(3) = 29.13$	<0.001	Kruskal-Wallis
	Lignin	$X^2(3) = 10.60$	<0.05	Kruskal-Wallis
	Lipid	$X^2(3) = 18.72$	<0.001	Kruskal-Wallis
	N-containing	$X^2(3) = 4.73$	n.s.	Kruskal-Wallis
	phenol	$F(3,103) = 26.17$	<0.001	ANOVA
	unknown	$X^2(3) = 1.53$	n.s.	Kruskal-Wallis
Horizon	aromatic	$F(4, 49.04) = 18.98$	<0.001	Welch's t-test
	carbohydrate	$X^2(4) = 32.51$	<0.001	Kruskal-Wallis
	lignin	$X^2(4) = 50.95$	<0.001	Kruskal-Wallis
	Lipid	$X^2(4) = 14.09$	<0.01	Kruskal-Wallis
	N-containing	$X^2(4) = 14.00$	<0.01	Kruskal-Wallis
	phenol	$F(4, 49.04) = 1.33$	n.s.	Welch's t-test
	unknown	$F(4, 102) = 23.54$	<0.001	ANOVA

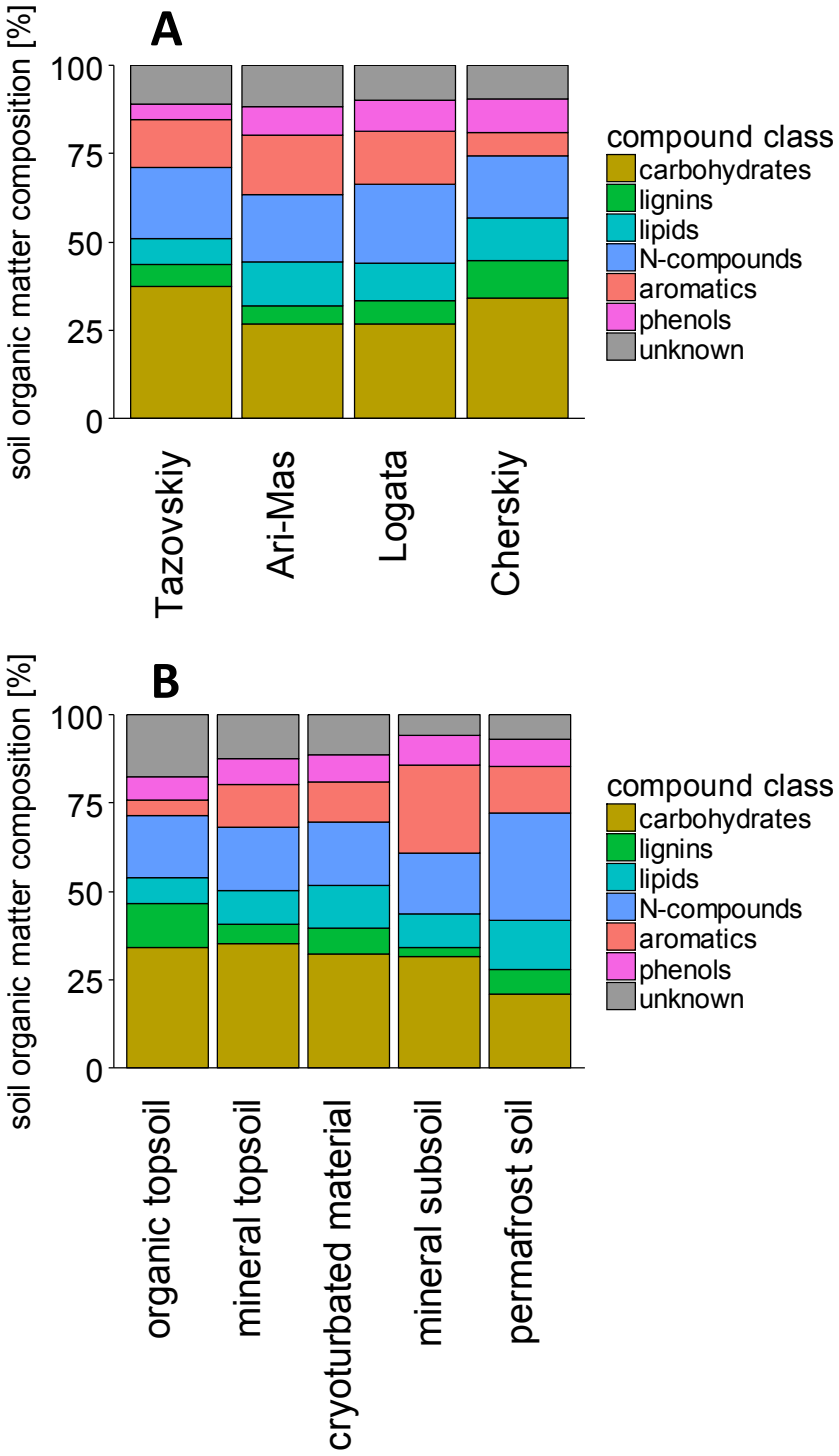

Fig. 1. **Soil organic matter composition of sites (A) and soil horizons (B).** The two bar chart displays the mean percentage of the six chemical compound classes that make up the soil organic matter in either the sites: Tazovskiy (n = 29), Ari-Mas (n = 29), Logata (n = 30) and Cherskiy (n = 18); or the horizons: organic topsoil (n = 18), mineral topsoil (n = 20), cryoturbated material (n = 26), mineral subsoil (n = 24) and permafrost (n = 18). Compounds that could not be assigned to a chemical class are reported as unknown.

Principal component analysis

To sidestep the issue of overfitting our models with too many compounds (n=151) relative to the observations (n=106), we performed a principal component analysis (PCA). This allowed us to reduce our 151-dimensional Py-GC/MS data into fewer linear axes that still described a maximum of the variance in our dataset (Fig. 2). The first three principal component axes PC1, PC2 and PC3 explained 21%, 14% and 7% of the variance in the data, respectively, and were further used as explanatory variables in our models.

The PCA results revealed that the sites Ari-Mas and Logata (both from Central Siberia) had a similar SOM composition across all three principal component axes (Fig. 2 A & D, Fig. 3 A & B & C). Moreover, the SOM composition of Tazovskiy (West Siberia) and Cherskiy (East Siberia) differed significantly from Ari-Mas and Logata across all three principal components (PC1: $x^2(3) = 28.82$, $p < 0.001$, Kruskal-Wallis; PC2: $F(3,102) = 18.82$, $p < 0.001$, ANOVA) (Fig. 3 A & B & C). Tazovskiy and Cherskiy, however, separated along the third principal component axis ($F(3,102) = 40.46$, $p < 0.001$, ANOVA).

Similar to sites, the SOM composition of soil horizons differed significantly along the PC1, separating mineral subsoil and permafrost soil from the other horizons ($F(4,101) = 12.84$, $p < 0.001$, ANOVA) (Fig. 2 B, Fig. 3 D). Likewise, there was a separation of soil horizons along the PC2 ($F(4,101) = 22.43$, $p < 0.001$, ANOVA), separating the mineral subsoil and permafrost soil from the mineral topsoil and cryoturbated material and the organic topsoil from all other horizons(Fig. 2 B, Fig. 3 E). Furthermore, along the PC3 we observed a separation of permafrost soil from cryoturbated material and mineral topsoil ($x^2(4) = 13.23$, $p < 0.05$, Kruskal-Wallis) (Fig. 2 E, Fig. 3 F).

Most importantly, the PCA plots enabled us to investigate the SOM composition of sites and horizons on a more detailed level (Fig. 2 C & F). Unlike Figure 1, the PCA results allowed us to distinguish soil samples not only by compound classes but also by the individual compounds that made up these compound classes.

A look at the principal component axes loadings underlying the PCA scores revealed that most pyrolysates had positive PC1 loadings, indicating a change in the diversity of pyrolysis products along the PC1 (Fig. 2 C, Fig. 3 G).

The SOM of observations with low PC1 scores was comprised of a higher number of different compounds in comparison to observations with high PC1 scores, whose SOM appeared to consist of fewer dominant compounds. Therefore, SOM of sites such as Ari-Mas and Logata was on average comprised of more diverse pyrolysis products than Tazovskiy and Cherskiy. Interestingly, the SOM composition in topsoils and in the cryoturbated material was more diverse than in the mineral subsoil and permafrost soil whose SOM composition was more uniform (Fig. 2 B & C, Fig. 3 D & G).

Furthermore, the separation of horizons along the PC2 coincided with a separation of chemical compound classes ($F(6,45.302) = 16.39$, $p < 0.001$, Welch's t-test) (Fig. 2 C, Fig. 3 H). The organic topsoil SOM consisted to a greater extent of carbohydrates and lignin derivatives, whereas the SOM in subsoils contained a higher amount of aromatic and phenolic compounds (Fig.2 B & C, Fig. 3 E & H). Additionally, aromatic compounds were relatively more abundant in Ari-Mas and Logata, whereas carbohydrates seemed to be relatively more common in Cherskiy and Tazovskiy (Fig. 2 B & C, Fig. 3 B & H).

The separation of Cherskiy and Tazovskiy along the PC3 was attributable to a separation of lipids from aromatic and unknown compounds ($F(6,144) = 4.37$, $p < 0.001$, ANOVA) (Fig. 2 F, Fig. 3 C & I), with a higher lipid content in Cherskiy versus a higher aromatic content in Tazovskiy. It was, however, not only the relative amounts in chemical compound classes that differed between the two sites. For instance, although the relative amount of carbohydrates was similar between Cherskiy and Tazovskiy, their most frequent carbohydrate compounds differed (Fig. 2 D & F).

Fig. 2

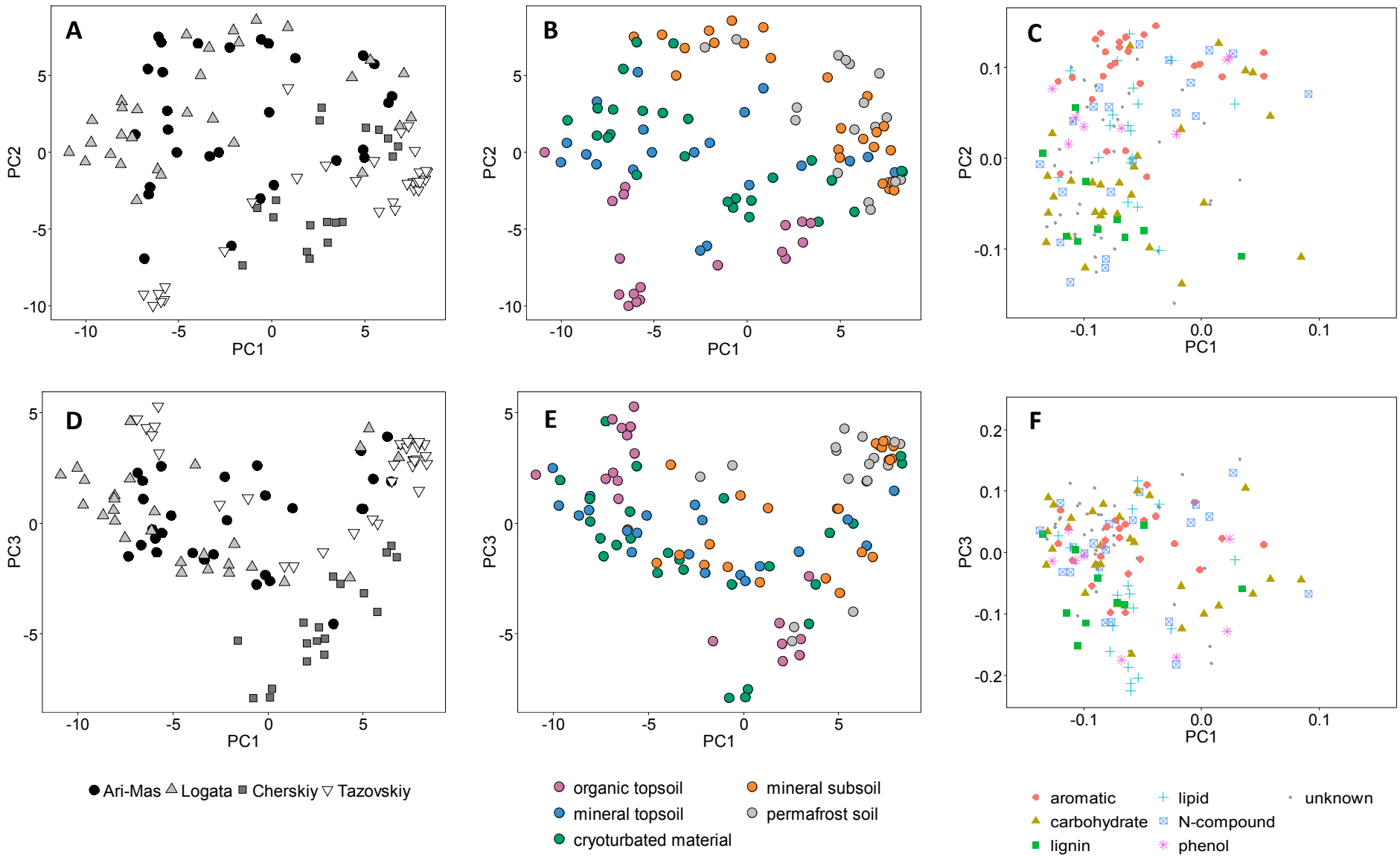
A
B
C
D
E
F
PC1
PC2
PC3
Ari-Mas
Logata
Cherskiy
Tazovskiy
organic topsoil
mineral topsoil
cryoturbated material
mineral subsoil
permafrost soil
aromatic
carbohydrate
lignin
lipid
N-compound
phenol
unknown

Fig. 3

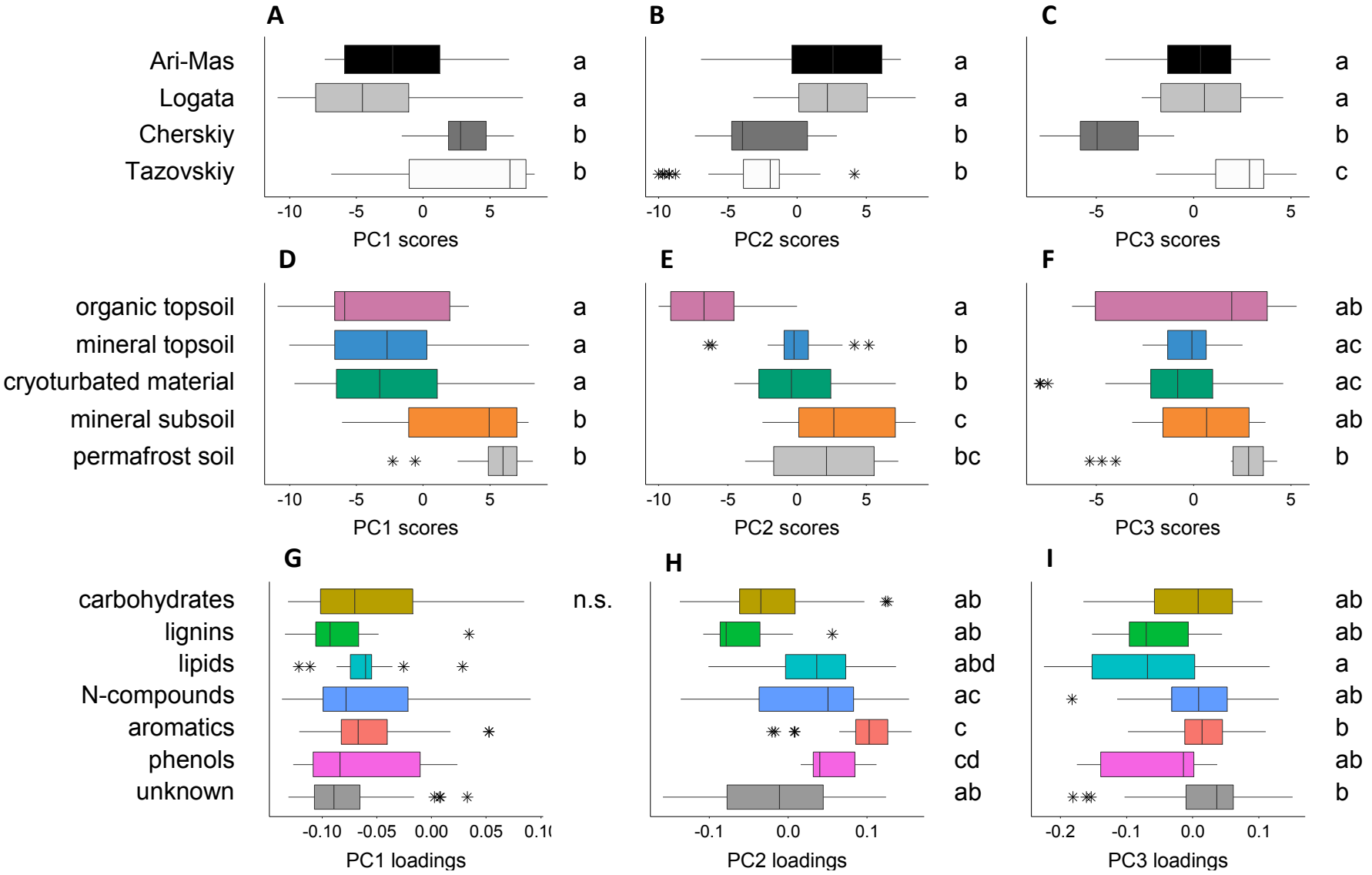
A
B
C
Ari-Mas
Logata
Cherskiy
Tazovskiy
a
a
b
b
a
a
b
b
a
a
b
c
-10 -5 0 5
PC1 scores
-10 -5 0 5
PC2 scores
-5 0 5
PC3 scores
D
E
F
organic topsoil
mineral topsoil
cryoturbated material
mineral subsoil
permafrost soil
a
a
a
b
b
a
b
b
c
bc
ab
ac
ac
ab
b
-10 -5 0 5
PC1 scores
-10 -5 0 5
PC2 scores
-5 0 5
PC3 scores
G
H
I
carbohydrates
lignins
lipids
N-compounds
aromatics
phenols
unknown
n.s.
ab
ab
abd
ac
c
cd
ab
ab
ab
a
ab
b
ab
b
-0.10 -0.05 0.00 0.05
PC1 loadings
-0.1 0.0 0.1
PC2 loadings
-0.2 -0.1 0.0 0.1
PC3 loadings

Fig. 2. **Sites and horizons differ in their soil organic matter composition.** Principal component analysis (PCA) of ranked pyrolysis-gas chromatography/ mass spectrometry data (Py-GC/MS). Panel A, B, D, E display the PCA scores for the first three principal component axes, while panel C and F display the PCA loadings. Panel A & D illustrate differences between sites: ● Ari-Mas, ▲ Logata, ■ Cherskiy, ▼ Tazovskiy. Panel B & E illustrate differences between horizons: ● organic topsoil, ● mineral topsoil, ● cryoturbated material, ● mineral subsoil, ● permafrost soil. Panel C & F display the six chemical compound classes: ▲ carbohydrates, ■ lignin derivatives, + lipids, ☒ N-containing, ● aromatics, ✳ phenols, ● unknown. Compounds that could not be assigned to a chemical class are depicted as grey dots ("unknown").

Fig. 3. **Separation of sites, horizons and compound classes along the first three principal component axes.** Boxes show medians and extend from the first quantile (Q1) to third quantile (Q3). Upper and lower whiskers are 1.5 times the length of the box and values outside this range are given as black stars. Panels A to C display box plots of PC1, PC2 & PC3 scores grouped by sites: Ari-Mas (n = 29), Logata (n = 30), Cherskiy (n = 18) and Tazovskiy (n = 29). Panels D to F show box plots of PC1, PC2 & PC3 scores grouped by horizon: organic topsoil (n = 18), mineral topsoil (n = 20), cryoturbated material (n = 26), mineral subsoil (n = 24) and permafrost (n = 18). Panels G to I display box plots of PC1, PC2 & PC3 loadings grouped by compound class: carbohydrates (n = 28), lignins (n = 10), lipids (n = 18), nitrogen-containing compounds (n = 21), aromatics (n = 26), phenols (n = 8) and unknown (n = 40). Letters next to the plots indicate significant differences ($p < 0.05$) as determined by ANOVA with subsequent Tukey HSD or by Welch test with subsequent pairwise t-test with Bonferroni correction.

Linear mixed effects model

In order to connect our results on the SOM composition with priming effect we used data from a previous study by Wild et al. (2016), specifically data of cumulative respiration (µmol C g^{-1} DW) and the priming effect expressed as response ratio (= respiration after substrate addition/ control respiration) after cellulose or protein addition. With these data, we performed three linear mixed models to predict variation in cumulative respiration (n = 106), cellulose priming (n = 101) and protein priming (n = 105) with the SOM composition represented by the first three principal component axes (PC1, PC2, PC3).

Cumulative respiration

The most parsimonious model to predict cumulative respiration contained the first three principal component axes (PC1, PC2, PC3) as explanatory variables and two-way interaction terms of PC1 and PC2 with *horizon* (Tab. S2). The interaction of the third principal component with *horizon* was removed from the model because it was not significant (Tab. 3), resulting in the final model formula:

respiration ~ PC1 + horizon + PC2 + PC3 + PC1:horizon + PC2:horizon

The significant interaction term implied that the effect of PC1 and PC2 on respiration differed between horizons, as illustrated in Figure 4. In general, respiration was highest in the organic topsoil, followed by a much lower respiration in the mineral topsoil and even lower respiration in the other horizons. In the organic topsoil PC1 and PC2 had a strong negative effect on respiration. In the mineral topsoil PC1 and PC2 had a weaker negative effect on respiration. Respiration in the cryoturbated material, the mineral subsoil, and permafrost soil was essentially unaffected by changes in PC1 and PC2. The PC3 had a weak positive effect on respiration in all horizons (Tab. S2, Fig. 4).

Tab. 3. Summary of initial and final linear mixed effects model, which explains respiration with the first three principal component axes and their interactions with soil horizons

fixed effects	numDf	denDf	AIC	LRT	Pr (>Chi)
Initial linear mixed effects model (BIC = -255.21)					
			-327.12		
PC1:horizon	4	63	-314.50	20.619	<0.001
PC2:horizon	4	63	-311.31	23.813	<0.001
PC3:horizon	4	63	-325.78	9.339	0.053
Final linear mixed effects model (BIC = -264.53)					
			-325.78		
PC3	1	67	-323.59	4.199	<0.05
PC1:horizon	4	67	-309.60	24.183	<0.001
PC2:horizon	4	67	-302.15	31.633	<0.001

Models were fitted by maximum likelihood. Statistical significance of explanatory terms was assessed by single-term deletions followed by likelihood ratio tests (LRT) between models including and excluding explanatory variables, with only significant terms were retained in the final model.
horizon factor with 5 levels: organic topsoil, mineral topsoil, mineral subsoil, cryoturbated material and permafrost soil
numDf numerator degree of freedom, *denDf* denominator degree of freedom,
AIC Akaike information criterion, *BIC* Bayesian information criterion, *LRT* likelihood ratio test

Priming effect after cellulose addition

In the model predicting cellulose priming, we excluded all three principal component axes and their two-way interaction terms with *horizon*, because they were not significant (Tab. 4). This resulted in a final model in which the cellulose priming was only explained by the factor *horizon* (Tab. S3).

cellulose priming ~ horizon

Consequently, the model resembled a one-way analysis of variance (ANOVA) and only enabled us to state differences in cellulose priming between soil horizons (Tab. S3, Fig. 5).

Tab. 4. Summary of initial and final linear mixed effects model, which explains cellulose priming with the first three principal component axes and their interactions with soil horizons

fixed effects	numDf	denDf	AIC	LRT	Pr (>Chi)
Initial linear mixed effects model (BIC = 230.68)					
			160.34		
PC1:horizon	4	57	155.34	3.004	0.557
PC2:horizon	4	57	152.58	0.246	0.993
PC3:horizon	4	57	154.39	2.051	0.726
Final linear mixed effects model (BIC = 170.14)					
			138.88		
horizon	4	72	146.21	15.335	0.004

Models were fitted by maximum likelihood. Statistical significance of explanatory terms was assessed by single-term deletions followed by likelihood ratio tests (LRT) between models including and excluding explanatory variables, with only significant terms were retained in the final model.
horizon factor with 5 levels: organic topsoil, mineral topsoil, mineral subsoil, cryoturbated material and permafrost soil
numDf numerator degree of freedom, *denDf* denominator degree of freedom,
AIC Akaike information criterion, *BIC* Bayesian information criterion, *LRT* likelihood ratio test

Priming effect after protein addition

The best fit model to explain protein priming contained all three principal component axes (Tab. S4). Moreover, it contained the significant two-way interaction terms of PC1 and PC3 with *horizon*. The non-significant interaction term between *horizon* with PC2 was removed from the model (Tab. 5), resulting in the final model formula:

protein priming ~ PC1 + horizon + PC2 + PC3 + PC1:horizon + PC3:horizon

The effect of PC2 on protein priming was a positive one across all horizons (Tab. S4, Fig. 6). In contrast, the effects of PC1 and PC3 differed between soil horizons (Tab. S4, Fig. 6). The PC1 affected protein priming strongly positive in the organic topsoil, the mineral topsoil, and the cryoturbated material. Generally, the cryoturbated material displayed higher protein priming than the organic topsoil or the mineral topsoil. In the permafrost soil and mineral subsoil, the effect of PC1 on protein priming was negative, but the effect was stronger negative in the permafrost soil. In the organic topsoil, we further found a strong positive effect of PC3. In all other horizons, PC3 affected protein priming negatively.

Tab. 5. Summary of initial and final linear mixed effects model, which explains protein priming with the first three principal component axes and their interactions with soil horizons

fixed effects	numDf	denDf	AIC	LRT	Pr (>Chi)
Initial linear mixed effects model (BIC = 139.91)					
			68.25		
PC1:horizon	4	66	75.96	15.705	0.003
PC2:horizon	4	66	66.54	6.290	0.178
PC3:horizon	4	66	73.48	13.230	0.010
Final linear mixed effects model (BIC = 127.68)					
			66.54		
PC2	1	66	70.29	5.747	0.017
PC1:horizon	4	66	80.41	21.868	<0.001
PC3:horizon	4	66	78.69	20.151	<0.001

Models were fitted by maximum likelihood. Statistical significance of explanatory terms was assessed by single-term deletions followed by likelihood ratio tests (LRT) between models including and excluding explanatory variables, with only significant terms were retained in the final model.
horizon factor with 5 levels: organic topsoil, mineral topsoil, mineral subsoil, cryoturbated material and permafrost soil
numDf numerator degree of freedom, *denDf* denominator degree of freedom,
AIC Akaike information criterion, *BIC* Bayesian information criterion, *LRT* likelihood ratio test

Discussion

There are still ambiguities regarding the mechanisms of rhizosphere priming (Heimann & Reichstein, 2008; Kuzyakov et al., 2000; Zhu et al., 2014). It is, however, clear that the priming effect is a microbial mediated process; therefore explanations so far are mainly based on microbial physiology such as an alleviation of energy and carbon limitations of microbial communities, a stimulation of microbial growth or mining for nutrients (E. Blagodatskaya & Kuzyakov, 2008; Craine et al., 2007; Dijkstra et al., 2013; Fontaine et al., 2003). Here we investigated whether SOM composition also affected the magnitude of heterotrophic respiration and the magnitude of the rhizosphere priming effect. Toward this end, we analyzed 106 soil samples from different soil horizons and tried to link their soil organic matter composition to priming and respiration analyzed in a previous incubation experiment on the same samples by Wild et al. (2016).

Native soil organic matter composition

We found evidence for the relative decline in carbon-containing compounds (e.g. carbohydrates, lignin derivatives) with a simultaneous relative increase in nitrogen-containing compounds with soil depth (Fig. 1 B). This was consistent with the decreasing C/N ratio from organic topsoil to mineral subsoil that Wild et al. (2016) had measured for the identical samples. The decreasing C/N ratio reflected the progressively processed state of the SOM with soil depth (Rumpel & Kögel-Knabner, 2011; Spohn et al., 2016). Lower carbon relative to nitrogen may be due to the respiration of organic carbon for energy production, which led to a depletion of organic carbon with simultaneous enrichment of nitrogen in the SOM (Spohn et al., 2016). Moreover, the higher degree of decomposition of SOM in deeper soil layers was supported by the high proportions of low-molecular-weight aromatic pyrolysis products found in the mineral subsoil and permafrost SOM, characteristic for highly degraded SOM (Carr et al., 2010).

In addition, we observed another change in SOM quality along the soil profile. Plant-derived organic matter (OM) contributed a higher proportion to the topsoil SOM than to the SOM in subsoil. We concluded this from the high

proportions to which the topsoil SOM consisted of lignins and 'unknown' compounds, which we suggest to originate from plant cell wall material. In contrast, SOM in subsoils appeared to consist largely of microbial-derived OM, which we conclude from the high amounts of phenol, methyl phenols and styrene which are associated with microbial residues (Carr et al., 2010; Nierop et al., 2001). Further, the low proportions of lignins in the subsoil horizons indicated that lignins were not stabilized but have undergone substantial degradation (Fig. 1 B) (Mikutta et al., 2006; Rumpel et al., 2004).

There is evidence that SOM in permafrost was even more processed than in mineral subsoil. A closer look at the SOM composition of the horizons revealed, that the aromatic contents increased strongly with depth until the mineral subsoil. In the permafrost soil, however, aromatic contents declined strongly and were in the range of mineral topsoil and cryoturbated material (Fig. 1 B). Additionally, the proportion to which the SOM consisted of nitrogen-containing compounds increased considerably from mineral subsoil to permafrost layer (Fig. 1 B). Apparently, aromatic compounds were degraded to a greater extent in permafrost layer than in mineral subsoil, which may be due to the extreme carbon limitation in long-term frozen material due to low but constant activity of microbes. This suggests that there were active microbes at temperatures below zero, as it was reported for permafrost soils (Nikrad et al., 2016).

Taken together, the lower C/N ratio and the higher proportion of microbial-derived OM in subsoils indicate highly processed SOM (Rumpel & Kögel-Knabner, 2011). This might have resulted from a reduced input of organic carbon in deeper soil layers, as evident by the low proportions of carbohydrates in permafrost soil (Fig. 1 B). In contrast, the high carbohydrate and lignin proportions of the topsoil organic matter illustrated the regular input of plant-derived organic material. The reduced input of organic carbon in subsoils was probably also associated with lower carbon contents and a lack of easily degradable carbon compounds. Instead, other SOM components, such as aromatic and phenolic compounds, dominated the subsoil SOM, indicating poor SOM quality.

Respiration and soil organic matter composition

Overall, we found that the SOM quality played a role for both the respiration and the 'primeability' and therefore may be important to explain the magnitude of the priming effect.

Our standardized LME model of the cumulative respiration showed that the effects of the SOM composition on respiration differed between horizons. We found that a shift in SOM composition (PC2) towards higher relative proportions of carbohydrates and lignins had a positive effect on the respiration in the topsoil horizons, with a stronger positive effect in the organic topsoil than in the mineral topsoil (Fig. 4, Tab. S2). This indicates that a higher respiration in topsoils was related to a higher supply of fresh plant material (e.g. carbohydrates, lignins, 'unknown' compounds). We suggest that plant-derived carbohydrates were an easily available source of carbon and energy (Dao et al., 2018), whose preferential decomposition lead to a decline in the carbohydrate contents (in % of SOM) with depth (Fig. 1 B). Our assumption of a degradation of plant material in the topsoil was also supported by the presence of carbohydrate compounds such as furans and furaldehyde, which are indicative for microbial degradation of high molecular weight polysaccharides (Carr et al., 2010; Kaal et al., 2007; Nierop et al., 2001; Schellekens et al., 2009).

Additionally, a higher diversity of pyrolysis products (PC1) was related to a higher respiration in topsoil horizons (Fig. 4, Tab. S2). Carr et al. (2010) had attributed a reduction in pyrolysate diversity to a selective loss of labile compounds. From this, we infer that respiration was lower in soils where SOM was more microbially processed and consisted of fewer easily degradable compounds.

In contrast to the topsoil horizons, differences in respiration within subsoil horizons and cryoturbated material were not affected by a change in SOM composition (PC1 & PC2) (Fig. 4, Tab. S2). However, as illustrated in Figure 4, the cumulative respiration of subsoils and cryoturbated material was in general much lower than that of the topsoils, with organic topsoil exhibiting the highest respiration of all horizons.

We attributed the low respiration in the subsoil to poor SOM quality that potentially may have limited SOM decomposition (Fontaine et al., 2007).

Compared to the topsoil horizons, the SOM in subsoils consisted of lower proportions of carbohydrates and therefore had much higher proportions of aromatic and nitrogen-containing compounds, reflecting the limited supply of easily degradable compounds and the highly processed state of SOM in deeper soil layers. Aromatic rings, such as benzene rings (Seo et al., 2009), need to be cleaved by oxidative enzymes (Capek et al., 2015; Sinsabaugh, 2010). However, to produce extracellular enzymes microorganisms have to invest high amounts of carbon and nitrogen. In the long run, the energy gained from the decomposition of complex SOM compounds such as aromatics might be too little for the microbial community to sustain activity (Fontaine et al., 2007). Consequently, not only SOM decomposition might have been reduced but also a bulk of the subsoil microbial community might have become inactive or dormant (Don et al., 2013), explaining the low respiration in subsoils.

The differences in the magnitude of the respiration between soil horizons also coincided with the soil organic carbon (SOC) content (%). On average, the organic topsoil had the highest SOC contents and the mineral subsoil and permafrost soil had the lowest SOC contents (Wild et al., 2016). The decline in SOC contents was also supported by the reduced allocation of plant-derived compounds into the deeper soil layers, which we had concluded from the change in SOM composition (Fig. 1). Consequently, we attributed the higher respiration in topsoil horizons not only to the relative higher proportions of (easily degradable) carbohydrates in the SOM but also to the overall higher SOC contents. Most importantly though, this emphasizes that SOM decomposition in subsoils was not only restricted due to poor SOM quality but also because the SOC contents were low. The lower SOC contents led to a physical disconnection of microbes and their substrates (Schmidt et al., 2011). As a result, the probabilities for the enzyme to meet the substrate and for the microbes to assimilate the decomposition products were lower (Don et al., 2013; Spohn et al., 2016). Consequently, SOM decomposition and therefore respiration were lower in subsoils with low carbon concentrations, because the costs for enzyme synthesis were too large compared to the energy gained (Don et al., 2013). This supports a general carbon and energy limitation of microbial activity in subsoils (Fontaine et al., 2007; Rumpel & Kögel-Knabner, 2011).

Interestingly, the respiration rate of the cryoturbated material was as low as that of subsoils, although its SOM composition and SOC content (Schnecker et al., 2014; Wild et al., 2016) were very similar to that of mineral topsoil. Similar to the subsoil horizons, the respiration of the cryoturbated material also unaffected by changes in SOM composition. Reduced decomposition rates in cryoturbated material had been reported previously and were attributed to a functional decoupling of the topsoil-derived SOM and the subsoil microbial community composition (Schnecker et al., 2014).

In summary, the results of our standardized LME model proposed that SOM quality only affected SOM mineralization in topsoil horizons where the supply with labile plant-derived organic compounds was sufficient to sustain microbial activity. In contrast, low concentrations and poor quality of subsoil organic matter constrained microbial activities, thus overrode the potential impact of SOM quality on mineralization.

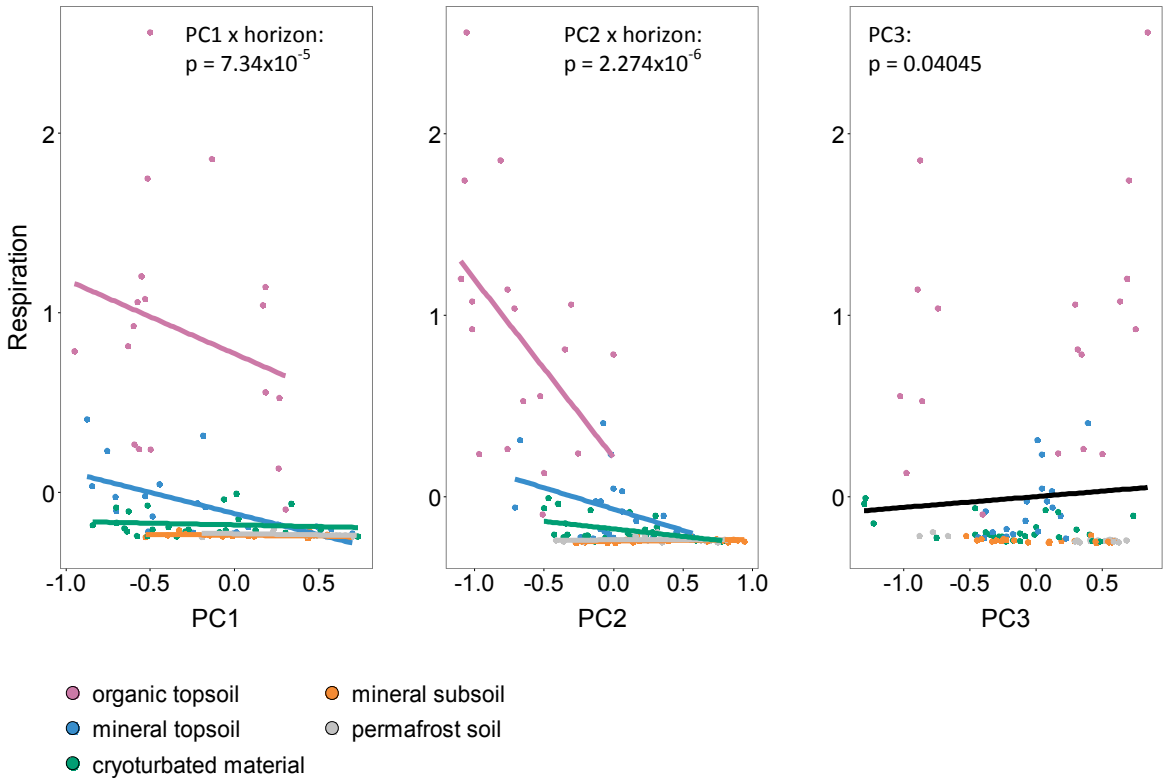

Fig. 4. **The relationship between respiration and soil organic matter.** The first three principal components (PC1, PC2, PC3) are used as a proxy for soil organic matter composition. Respiration data (µmol C g^{-1} DW) were normalized by mean subtraction and dividing by twice the standard deviation. Lines represent fit lines generated by standardized linear mixed effect model predicting different effects of PC1 and PC2 on respiration per horizon: — organic topsoil, — mineral topsoil, — mineral subsoil, — cryoturbated material, — permafrost soil. The effect of PC3 on respiration was positive across all horizons.

Priming effect and soil organic matter composition

We found that the variation in the magnitude of the priming effect was related to the native SOM composition. However, we discovered that this relationship was dependent on the added substrate, which was either an organic carbon only (cellulose) or an organic nitrogen source (protein), containing organic C and N.

With our standardized LME model for the cellulose priming effect, we could not detect a relationship of SOM composition and priming effect by the addition of an organic carbon source (Fig. 5, Tab. 3). Our model demonstrated differences in the cellulose priming between horizons but did not contribute further information on what caused them (Fig. 5). We can, however, conclude that the variables describing the SOM composition (PC1, PC2, PC3) failed to explain variation in cellulose priming, and therefore had been removed from the model in the course of the variable selection (Tab. 3). The differences in priming effect may have been caused by the different microbial community composition of the soil horizons (Schnecker et al., 2015) or other unknown factors.

However, we cannot rule out that our standardized LME model explaining the priming response to cellulose addition has failed to demonstrate an existing relationship to SOM composition because the Py-GC/MS measurements, followed by a reduction of the data into three principal component axes, failed to capture the SOM properties relevant to the priming effect. Furthermore, the variation in the priming effect was lower for the cellulose than for the protein amended soils, which might have played a role as well.

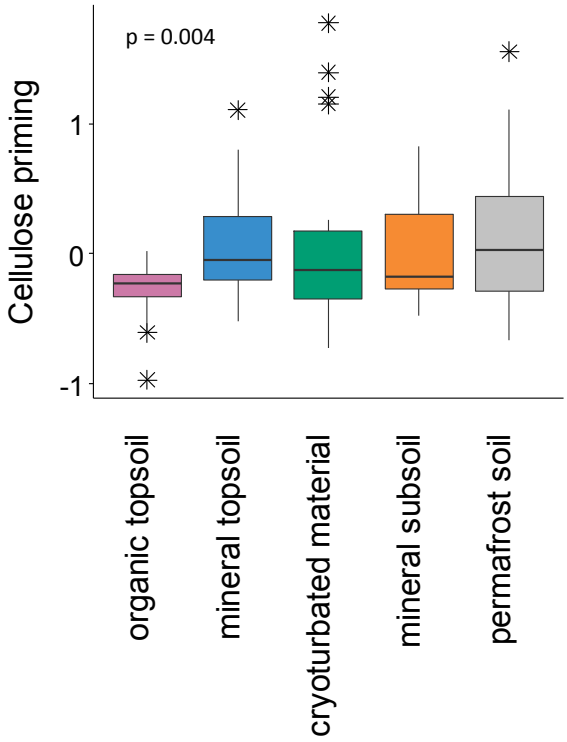

Fig. 5. **The relationship between cellulose priming and soil organic matter.** Cellulose priming could not be explained by soil organic matter composition (PC1, PC2, PC3) and we could only determine differences in cellulose priming between horizons. As such, box plots show medians and extend from the first quantile (Q1) to third quantile (Q3), with upper and lower whiskers being 1.5 times the length of the box and values outside this range being given as black stars.

In contrast, the standardized LME model explaining the protein priming effect demonstrated a relationship between SOM composition and the magnitude of the priming effect (Fig. 6, Tab. 4).

We found that across all horizons the priming effect by protein addition was the greater the higher the proportion was, to which the SOM consisted of aromatic and phenolic compounds (poor SOM quality). Therefore, the subsoils with their high aromatic contents showed the strongest protein priming. On the other hand, the priming effect was lowest in soils rich in carbohydrates and lignins (plant derived compounds), which was particularly true in the topsoil horizons.

We attributed the stronger response in soils with higher aromatic and phenolic contents, such as the subsoil horizons, to the fact that the aromatic fraction of the SOM cannot be efficiently decomposed due to its poor quality. This was certainly also reinforced by the low SOC contents in the subsoil horizons (Wild et al., 2016). This can be concluded from the low respiration of subsoil horizons illustrated in the LME model describing the respiration (Fig. 4). The supply with protein might have alleviated the energy limitation caused by the poor SOM quality (and low SOC content) and allowed the microorganisms to decompose the complex SOM (Fontaine et al., 2007). However, the alleviation of the microbial energy limitation cannot be the sole reason for the observed priming effect. If that had been the case, a supply of cellulose should have had similar effects and we would have seen this relationship also in our LME model explaining cellulose priming.

We propose that instead the organic nitrogen provided by the protein addition, played a key role in the relationship between the SOM composition and the priming effect. Studies have shown, that an addition of both carbon and nitrogen alleviated prevailing stoichiometric constraints and lead to increased enzyme production (Chen et al., 2014; Drake et al., 2013; Wild et al., 2016). We also suggest that the microbial community might have invested the additional nitrogen obtained from the protein into the synthesis of extracellular enzymes (Allison et al., 2009; Craine et al., 2007), needed for the degradation of aromatic compounds (Seo et al., 2009), which may have stimulated the breakdown of complex SOM (Schimel & Weintraub, 2003). Wild et al. (2014) came to similar conclusions when incubating identical soils with an addition of protein. Nitrogen

demands required for microbial growth and priming effect were better met by adding a carbon and nitrogen containing substrate (Drake et al., 2013).

In contrast, the priming effect was lowest in soils rich in carbohydrates and lignins such as the topsoil horizons (Fig. 6). In these soils, the low priming effect came alongside with high respiration rates (Fig. 4). We had attributed this to the high carbohydrate contents of these soil that provided enough easily degradable compounds so that the microbial community did not suffer energy or carbon limitations. Therefore, the response to a substrate addition was much weaker. That the protein addition in topsoil horizons nevertheless led to a priming effect can be attributed to a possible nitrogen-limited of these soils (Wild et al., 2014, 2016). SOM in soils with weak priming effects consisted in addition to the high carbohydrate proportions also of high lignin proportions. Somewhat surprisingly, the high contents of lignin derivatives, which are chemically speaking also aromatics, did not lead to higher protein priming, as did the high aromatic and phenolic contents in the subsoil. This could have been caused by a more limited degradation of lignin than of other aromatic compounds. This reduced degradation might be related to its complex three-dimensional network of non-phenolic phenylpropanoid units linked by resistant carbon-carbon and ether bonds. This bulky molecular architecture reduces the accessibility for enzymes and thereby limits degradation. Additionally, specialized peroxidases are needed to degrade lignins which are mainly produced by a small group of ligninolytic fungi (Dao et al., 2018; Ruiz-Dueñas & Martínez, 2009).

We propose that the relationship of priming effect and SOM composition only became apparent when additional nitrogen promoted the production of extracellular enzymes, leading to an increase in native SOM degradation. The priming effect was stronger in soils with poor SOM quality characterized by a high proportion of compounds that needed extracellular enzymes for breakdown but whose SOM degradation did not provide enough net energy gain to sustain high microbial activities.

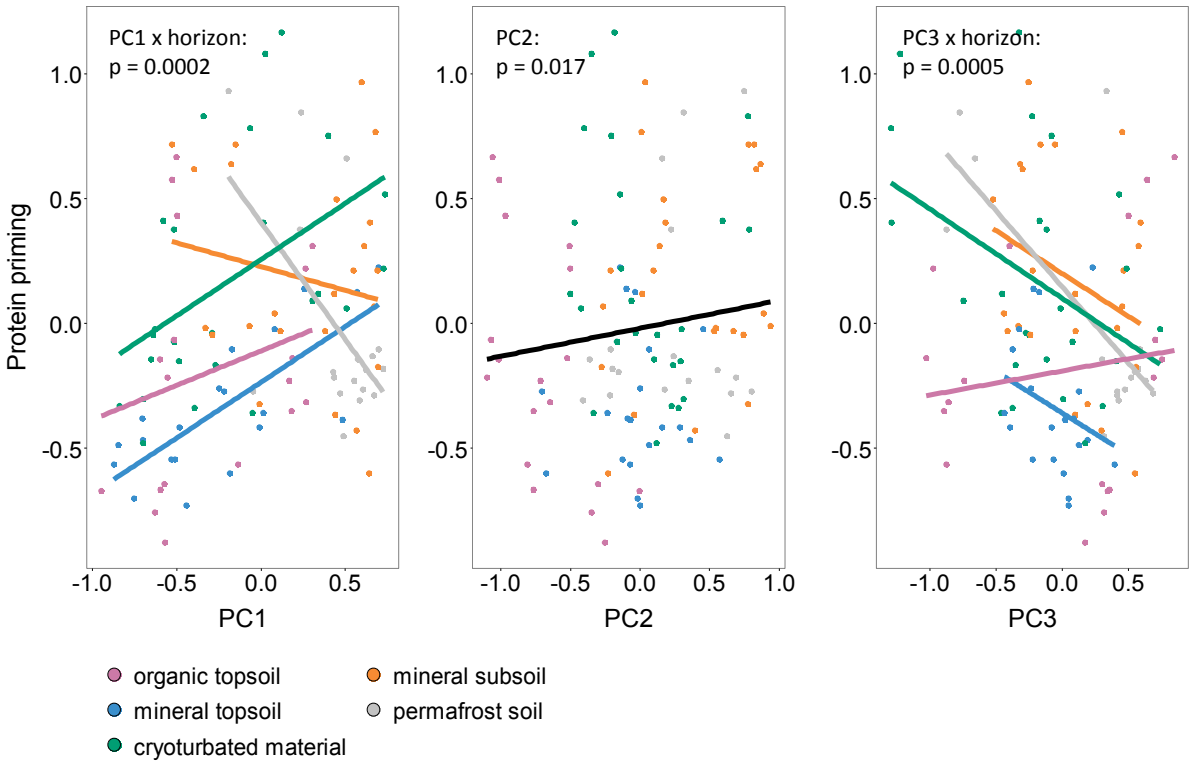

Fig. 6. **The relationship between protein priming and soil organic matter.** The first three principal components (PC1, PC2, PC3) are used as a proxy for soil organic matter composition. Lines represent fit lines generated by standardized linear mixed effects model predicting different effects of PC1 and PC3 on protein priming per horizon: — organic topsoil, — mineral topsoil, — mineral subsoil, — cryoturbated material, — permafrost soil. The effect of PC2 on protein respiration was positive across all horizons.

In summary, we have shown that native SOM composition can explain differences in both the respiration and the priming effect in permafrost soils. Similar to what we had hypothesized, the respiration was lowest in soils with poor SOM quality, which was characterized by high proportions of aromatic and phenolic compounds. This was true for subsoil horizons where microbial activity was reduced due to energy limitation induced by poor SOM quality and low SOC contents. In contrast, respiration was highest in soils that were rich in easily degradable compounds, such as carbohydrates. This was the case in the topsoil horizons that received a regular input of plant-derived organic compounds.

Our standardized LME models suggest that the relationship between SOM composition and priming effect only exists when an organic nitrogen source (protein) is added, but not for an organic carbon source alone (cellulose). This suggests that the alleviation of the energy limitation of the soil microbes is not enough to establish a relationship between priming effect and SOM composition. We propose that this relationship only becomes apparent when additional nitrogen promotes the production of extracellular enzymes, leading to an increase in native SOM degradation. Accordingly, protein addition caused the strongest response in soils with poor SOM quality as it enables the decomposition of complex SOM, such as the aromatic SOM fraction, whose efficient degradation was not possible prior to substrate addition.

Supplement

Tab. S1. List of identified pyrolysis-gas chromatography/ mass spectrometry (Py-GC/MS) products containing product formula, product name, specific mass fragments (m/z) and average retention time (RT)

Formula	Name	m/z	RT
Lipids (18 compounds)			
$C_{12}H_{24}$	Dodecane	57, 43, 71	7.6
$C_{13}H_{28}$	Tridecane	57, 43, 71	9.44
$C_{14}H_{30}$	Tetradecane	57, 43, 71	11.3
$C_{15}H_{32}$	Pentadecane	57, 43, 71	13.12
$C_{16}H_{34}$	Hexadecane	57, 43, 71	14.87
$C_{17}H_{36}$	Heptadecane	57, 43, 71	16.56
$C_{18}H_{38}$	Octadecane	57, 43, 71	18.17
$C_{19}H_{40}$	Nonadecane	57, 43, 71	19.56
$C_{12}H_{24}$	Dodecene	55, 41, 43	8.42
$C_{13}H_{26}$	Tridecene	55, 41, 43	10.37
$C_{14}H_{28}$	Tetradecene	55, 41, 43	12.15
$C_{15}H_{30}$	Pentadecene	55, 41, 43	13.83
$C_{16}H_{32}$	Hexadecene	55, 41, 43	15.69
$C_{17}H_{34}$	Heptadecene	55, 41, 43	17.35
$C_{18}H_{36}$	Octadecene	55, 41, 43	19.08
$C_{19}H_{38}$	Nonadecene	57, 83, 97	20.39
$C_{20}H_{40}$	Eicosene	97, 57, 83	22.02
$C_{21}H_{42}$	Heneicosene	55, 41, 43	23.15
Aromatics & polyaromatics (26 compounds)			
C_8H_{10} / C_5H_8O	p-Xylene / Cyclopentanone	91, 106, 105 / 55, 28, 84	7.46
C_9H_{12}	Benzene, 1-ethyl-3-methyl-	105, 120, 91	8.18
C_8H_8	Styrene	104, 103, 78	8.76
C_9H_{12}	Benzene, 1-ethyl-2-methyl-	105, 120, 91	8.87
C_9H_{12}	Mesitylene	105, 120, 119	9.26
$C_{10}H_{14}$	Benzene, (2-methylpropyl)-*	91, 92, 134	9.79
C_9H_{10}	α-Methylstyrene*	118, 117, 103	10.16
C_9H_{12}	Benzene, 1-ethyl-3-methyl-	105, 120, 91	10.29
C_9H_{10}	Indane	117, 118, 115	10.69
C_9H_{10}	Indane	117, 118, 115	11.53
C_9H_8	Indene	116, 115, 89	13.01
C_7H_6O	Benzaldehyde	77, 106, 105	13.68
$C_{10}H_{10}$	2-Methylindene*	130, 115, 129	15.04
$C_{10}H_{10}$	1H-Indene, 3-methyl-*	130, 115, 129	15.2
C_8H_8O	Phthalan	91, 92, 120	15.45
$C_{14}H_{22}$	Benzene, octyl-*	91, 92, 190	17.2
$C_{10}H_8$	Naphthalene	128, 129,127	17.47
$C_{16}H_{26}$	Benzene, (1-ethyloctyl)-*	91, 119, 105	17.96
$C_{11}H_{10}$	Naphthalene, 2-methyl-	142, 141, 115	19.71
C_8H_7N	Benzyl nitrile	117, 116, 90	20.24
$C_{12}H_{12}$	Naphthalene, 1,7-dimethyl-*	156, 141, 155	20.84
$C_{12}H_{12}$	Naphthalene, 1,4-dimethyl-*	156, 141, 155	21.37

C_9H_8O	1H-Inden-1-one, 2,3-dihydro-	104, 132, 103	21.54
$C_{13}H_{14}$	Naphthalene, 1,4,6-trimethyl-	155, 170, 153	23.79
$C_{10}H_{10}O_2$	6-Methoxy-3-methylbenzofuran*	147, 162, 91	27.02
$C_{10}H_{10}O_2$	6-Methoxy-3-methylbenzofuran*	147, 162, 91	27.25

Carbohydrates (28 compounds)

C_5H_6O	Furan, 2-methyl-	82, 53, 81	8.08
$C_3H_6O_2$	2-Propanone, 1-hydroxy-	43, 31, 74	9.61
C_5H_6O	2-Cyclopenten-1-one*	82, 39, 54	10.59
C_6H_8O	2-Cyclopenten-1-one, 2-methyl-	67, 96, 53	10.84
$C_5H_4O_2$	3-Furaldehyde	95, 96, 39	11.90
$C_5H_6O_2$	2(3H)-Furanone, 5-methyl-	55, 98, 43	12.04
$C_7H_{10}O$	2-Cyclopenten-1-one, 2,3-dimethyl-	67, 110, 39	12.31
$C_5H_4O_2$	Furfural	96, 95, 39	12.56
$C_6H_6O_2$	Ethanone, 1-(2-furanyl)-	95, 110, 39	13.31
C_8H_6O	Benzofuran	118, 90, 89	13.36
C_6H_8O	2-Cyclopenten-1-one, 3-methyl-	96, 67, 53	13.58
$C_5H_6O_2$	2H-Pyran-2-one, 5,6-dihydro-	68, 39, 40	13.84
$C_7H_{10}O$	2-Cyclopenten-1-one, 2,3-dimethyl-	67, 110, 39	13.96
$C_6H_6O_2$	2-Furancarboxaldehyde, 5-methyl-	110, 109, 53	14.52
$C_5H_6O_2$	2(5H)-Furanone, 5-methyl-	55,98, 43	16.34
$C_5H_6O_2$	2(5H)-Furanone, 3-methyl-*	41, 69, 39	16.98
$C_6H_6O_2$	1,4-Cyclohex-2-enedione*	54, 82, 110	17.28
C_2H_5NO	Acetamide	59, 44, 43	17.58
C_6H_8O2	2-Cyclopenten-1-one, 2-hydroxy-3-methyl-	112, 69, 55	18.64
$C_6H_8O_3$	2,4(3H,5H)-Furandione, 3-ethyl-*	55, 70, 100	20.66
$C_6H_6O_3$	Maltol	126, 71, 43	20.73
$C_6H_6O_3$	Levoglucosenone	98, 96, 39	21.15
$C_{17}H_{30}O$	2-Tridecylfuran*	81, 95, 82	23.27
$C_6H_8O_4$	1,4:3,6-Dianhydro-α-d-glucopyranose	69, 29, 57	23.48
C_8H_8O	Benzofuran, 2,3-dihydro-	120, 91, 119	26.42
$C_6H_8O_4$	1,4:3,6-Dianhydro-α-d-glucopyranose	69, 29, 57	26.52
$C_6H_7NO_2$	3-Acetamidofuran	83, 43, 125	27.25
$C_6H_6O_3$	5-Hydroxymethylfurfural	97, 126, 41	27.72

Lignin derivatives (10 compounds)

$C_6H_6O_2$	Resorcinol	110, 82, 81	16.45
$C_7H_8O_2$	Phenol, 2-methoxy-	109, 124, 81	19.16
$C_8H_{10}O_2$	Creosol	138, 123, 95	20.61
$C_9H_{12}O_2$	Phenol, 4-ethyl-2-methoxy-	137, 152,15	21.68
$C_{10}H_{12}O_2$	Eugenol	164, 103, 77	23.57
$C_9H_{10}O_2$	2-Methoxy-4-vinylphenol	135, 150, 107	23.96
$C_8H_{10}O_3$	Phenol, 2,6-dimethoxy-	154, 139, 111	24.83
$C_{10}H_{12}O_2$	trans-Isoeugenol	164, 149, 103	25.92
$C_8H_{10}O_2$	3-Methoxy-5-methylphenol	138, 109, 107	27.99
$C_{20}H_{28}O_{13}$	Vanillin lactoside*	152, 151, 81	28.59

Phenols (8 compounds)

C_6H_6O	Phenol	94, 66, 65	11.7
C_8H_8O	Acetophenone	105, 77, 51	15.87
$C_8H_{10}O$	Phenol, 2-ethyl-	107, 122, 77	22.19
C_7H_8O	Phenol, 4-methyl-	107, 108, 77	22.35
C_7H_8O	Phenol, 3-methyl-	108, 107, 79	22.46

$C_8H_{10}O$	Phenol, 4-ethyl-	107, 122, 77	23.63
$C_8H_{10}O$	Phenol, 3-ethyl-	107, 122, 77	23.72
$C_8H_{10}O$	Phenol, 3,4-dimethyl-	107, 122, 121	24.22
Nitrogen-containing compounds (21 compounds)			
C_5H_5N	Pyridine	79, 52, 51	7.28
C_9H_{12} / C_6H_7N	Benzene, propyl- / Pyridine, 2-methyl-	91, 120, 92 / 93, 66, 92	7.90
C_6H_7N	Pyridine, 4-methyl-	93, 66, 92	9.30
C_6H_7N	Pyridine, 3-methyl-	93, 66, 92	9.33
	Pyrrolidine, 2-butyl-1-methyl-		12.65
C_4H_5N	Pyrrole	67, 39, 41	13.44
C_5H_7N	1H-Pyrrole, 3-methyl-	80, 81, 53	14.12
C_7H_5N	Benzonitril	103, 76, 50	14.13
C_5H_7N	1H-Pyrrole, 3-methyl-	80, 81, 53	14.42
C_9H_8O / C_6H_9N	Benzofuran, 2-methyl- / 1H-Pyrrole, 2,3-dimethyl-	131, 132, 77 / 94, 95, 80	14.94
C_6H_9N	1H-Pyrrole, 3-ethyl-*	80, 95, 53	15.22
C_6H_9N	1H-Pyrrole, 2-ethyl-*	80, 95, 94	16.02
$C_8H_{19}N$	N-Butyl-tert-butylamine*	114, 58, 30	19.33
C_5H_5NO	1H-Pyrrole-2-carboxaldehyde	95, 94, 66	21.58
C_9H_9N	Benzenepropanenitril	91, 131, 65	21.92
$C_8H_{11}NO$	Benzenamine, 3-ethoxy-*	109, 139, 80	22.15
C_5H_5NO	3-Pyridinol*	95, 39, 40	26.68
C_8H_7N	Indole	117, 90, 89	27.13
$C_4H_5NO_2$	Succinimide	99, 28, 56	27.44
C_9H_9N	Indole, 3-methyl-	130, 131, 77	27.65
	1H-Pyrrole-2-carbonitrile*		27.81

* compound was assigned to the chemical class based on structural similarities to other compounds in the compound class, which makes a similar source plausible.
40 of the 151 compounds could not be identified by their mass spectra and are not included in the table.

Tab. S2. Parameter estimates and 95% confidence intervals of the final mixed effects model explaining cumulative respiration. Confidence intervals were acquired by normal approximation to the distribution of the maximum likelihood estimators.

respiration ~ PC1 + horizon + PC2 + PC3 + PC1:horizon + PC2:horizon			
Fixed effects	lower 95% CI	estimate	upper 95% CI
(Intercept)	-0.189	-0.129	-0.068
PC1	-0.381	-0.264	-0.147
Mineral subsoil	-0.166	-0.104	-0.043
Permafrost	-0.165	-0.105	-0.044
Cryoturbated material	-0.129	-0.065	-0.002
Organic topsoil	-0.461	0.197	0.855
PC2	-0.478	-0.300	-0.122
PC3	-0.021	-0.012	-0.004
PC1:mineral subsoil	0.135	0.253	0.371
PC1:permafrost	0.144	0.262	0.380
PC1:cryoturbated material	0.048	0.176	0.304
PC1:organic topsoil	-0.857	-0.190	0.477
PC2:mineral subsoil	0.108	0.287	0.466
PC2:permafrost	0.127	0.305	0.484
PC2:cryoturbated material	-0.026	0.163	0.353
PC2:organic topsoil	-1.545	-0.701	0.142

Tab. S3. Parameter estimates and 95% confidence intervals of the final mixed effects model explaining cellulose priming. Confidence intervals were acquired by normal approximation to the distribution of the maximum likelihood estimators.

cellulose priming ~ horizon			
Fixed effects	lower 95% CI	estimate	upper 95% CI
(Intercept)	-0.144	0.039	0.221
Mineral subsoil	-0.297	-0.062	0.172
Permafrost	-0.212	0.113	0.438
Cryoturbated material	-0.275	0.034	0.344
Organic topsoil	-0.540	-0.331	-0.122

Tab. S4. Parameter estimates and 95% confidence intervals of the final mixed effects model explaining protein priming. Confidence intervals were acquired by normal approximation to the distribution of the maximum likelihood estimators.

protein priming ~ PC1 + horizon + PC2 + PC3 + PC1:horizon + PC3:horizon			
Fixed effects	lower 95% CI	estimate	upper 95% CI
(Intercept)	-0.385	-0.210	-0.035
PC1	0.046	0.215	0.384
Mineral subsoil	0.135	0.334	0.533
Permafrost	0.290	0.548	0.807
Cryoturbated material	0.258	0.419	0.581
Organic topsoil	0.276	0.593	0.911
PC2	0.066	0.237	0.408
PC3	-0.268	0.012	0.292
PC1:mineral subsoil	-0.657	-0.238	0.181
PC1:permafrost	-1.326	-0.853	-0.381
PC1:cryoturbated material	-0.230	0.076	0.382
PC1:organic topsoil	0.626	1.382	2.139
PC3:mineral subsoil	-0.836	-0.332	0.172
PC3:permafrost	-0.765	-0.352	0.060
PC3:cryoturbated material	-0.698	-0.303	0.092
PC3:organic topsoil	0.498	0.981	1.464

PART 3

Summary

Temperatures are rising twice as fast in higher latitudes than they do on the global average. As a consequence, plant productivity in Arctic regions is increasing, which in turn implies an increased belowground carbon allocation in the form of rhizodeposits. These labile carbon compounds may stimulate soil organic matter (SOM) decomposition by a process called 'rhizosphere priming effect'. As a consequence, carbon dioxide (CO_2) might be released from permafrost soils to the atmosphere where it might lead to a positive feedback to climate change. There are still many ambiguities regarding mechanisms and controls of the priming effect. It was suggested that the direction and the extent of the priming effect are influenced by the microbial activity, biomass and community composition as well as the amount and quality of the added substrate. In addition, the native SOM composition may also affect rhizosphere priming.

The overall aim of this study was to assess if the rhizosphere priming effect was affected by the native SOM composition. Expecting that SOM quality plays an important role for heterotrophic respiration and rhizosphere priming, we hypothesized (1) that complex organic matter (i.e. OM that requires more enzymatic steps to be broken down) will result in lower respiration rates than SOM with higher proportion of easily assimilable compounds. Additionally, we hypothesized (2) that the priming effect would be higher in soil where soil organic matter consisted to a greater extent of complex compounds and compounds which breakdown products may be potentially toxic to microbes (e.g., aromatics and phenols), compared to soils containing higher proportions of easily degradable compounds (e.g., plant-derived carbohydrates).

Because the production of extracellular enzymes that are ultimately responsible for a priming effect requires carbon and nitrogen, we tested whether the addition of carbon (cellulose) alone or carbon in combination with nitrogen (protein) would differentially affect the relationship between soil organic matter and priming. Our dataset encompassed 106 soil samples from five soil horizons from four permafrost sites across Siberia. Data on respiration and priming effect

were obtained from a previous study in which identical samples were incubated under similar conditions with cellulose or protein addition to assess the priming effect. We determined the SOM composition by pyrolysis-gas chromatography/mass spectrometry (Py-GC/MS). We performed standardized linear mixed effects (LME) models to explain the variation in both the respiration and the priming effect with SOM composition. Py-GC/MS data were reduced into several linear axes by principal component analysis (PCA) and the first three PCs (representing SOM composition) were used as explanatory variables in the standardized LME models.

Our Py-GC/MS data indicate that with increasing soil depth, the SOM was increasingly processed. The decline of carbohydrate and lignins with the simultaneous increase in aromatic and phenolic compounds illustrates the decrease in SOM quality with soil depth. We concluded that topsoil SOM was made up to a large extent of plant-derived organic material, whereas subsoil SOM consisted largely of microbial-derived compounds.

Our standardized LME model of respiration showed that in topsoils the respiration was highest in soils with a high amount of carbohydrates and lignins while subsoil respiration was not affected by a change in SOM composition. From this, we conclude that the SOM quality only affected SOM mineralization in topsoil horizons where there was a steady supply of labile plant-derived compounds.

Our standardized LME models also revealed that SOM composition affected the magnitude of the priming effect. However, this relationship was dependent on the added substrate. We found that the SOM composition failed to explain the variation in the priming effect caused by the addition of organic carbon (cellulose) alone. This suggests that an alleviation of a potential microbial energy limitation does not alone explain a relationship between SOM and respiration. In contrast, when we added organic nitrogen (protein) we found that the priming effect was highest in soils with poor SOM quality, characterized by high aromatic and phenolic contents. The addition of a carbon and nitrogen containing substrate (protein) might have better met the microbial demands for growth. Further, the additional nitrogen might have been invested into the production of extracellular enzymes, allowing for the degradation of the aromatic

and phenolic fraction of the SOM that could not be decomposed prior to substrate addition, due to a lack in sufficient extracellular enzymes.

With our study, we could show that the native SOM composition has an effect on both the respiration and the magnitude of the priming effect. However, we propose that additional organic nitrogen plays a crucial role for this relationship to become visible. The SOM composition only exerts its influence on the priming effect when microbes are provided with both carbon and nitrogen.

Zusammenfassung

Die Temperaturen steigen in höheren Breiten doppelt so schnell wie im globalen Durchschnitt. Als Folge davon nimmt die Pflanzenproduktivität in arktischen Regionen zu, was wiederum zu einem erhöhten Transport von Kohlenstoff in Form von Rhizodepositen in den Boden führt. Diese labilen Kohlenstoffverbindungen können die Zersetzung organischer Substanz im Boden durch den sogenannten "Rhizosphären-Priming-Effekt" stimulieren. Das könnte dazu führen das Kohlendioxid (CO_2) aus Permafrostböden in die Atmosphäre freigesetzt wird, wo es zu einer positiven Rückkopplung auf den Klimawandel beitragen könnte. Nichtsdestotrotz gibt es immer noch viele Unklarheiten bezüglich der Mechanismen und Kontrollen des Priming-Effekts. Es wird angenommen, dass die Richtung und das Ausmaß des Priming-Effekts durch die Biomasse und Zusammensetzung der mikrobiellen Gemeinschaft sowie durch die Qualität und Quantität des zugegebenen Substrats beeinflusst wird. Darüber hinaus könnte auch die Zusammensetzung der organischen Substanzen im Boden den Rhizosphären-Priming-Effekt beeinflussen.

Das Ziel dieser Studie war es herauszufinden, ob der Rhizosphären-Priming-Effekt durch die Zusammensetzung des bodeneigenen organischen Materials beeinflusst wird. Da wir erwarteten, dass die Qualität des organischen Materials im Boden eine wichtige Rolle bei der heterotrophen Respiration und dem Rhizosphären-Priming-Effekt spielt, nahmen wir an (1), dass komplexe organische Substranzen (d.h. organisches Material, das mehr enzymatische Schritte erfordert) zu niedrigeren Respirationsraten führen würden als organisches Material mit einem höheren Anteil an leicht assimilierbaren Verbindungen. Darüber hinaus stellten wir die Hypothese auf (2), dass der

Priming-Effekt in Böden höher ist, in denen die organische Bodensubstanz zu einem größeren Teil aus komplexen Verbindungen und Verbindungen, deren Abbauprodukte potenziell toxisch für Mikroben sind (z.B. Aromaten und Phenole), besteht, verglichen mit Böden, die hohe Mengen leicht abbaubarer Verbindungen enthalten (z.B. pflanzliche Kohlenhydrate).
Da die Produktion von extrazellulären Enzymen, die letztlich für einen Priming-Effekt verantwortlich sind, Kohlenstoff und Stickstoff erfordert, testeten wir, ob die Zugabe von Kohlenstoff (Cellulose) allein oder Kohlenstoff in Kombination mit Stickstoff (Protein) die Beziehung zwischen organischer Bodensubstanz und Priming-Effekt beeinflussen würde.

Unser Datensatz umfasste 106 Bodenproben aus fünf Bodenhorizonten von vier Permafrostböden aus Sibirien. Die Daten zum Priming-Effekt und zur Respiration stammen aus einer früheren Studie, in der identische Proben unter gleichen Bedingungen mit Cellulose- oder Protein-Zugabe sowie ohne Substratzugabe inkubiert wurden. Wir bestimmten die Zusammensetzung der organischen Bodensubstanz durch Pyrolyse-Gaschromatographie/ Massenspektrometrie (Py-GC/MS). Wir führten standardisierte lineare Mixed-Effect (LME) Modelle durch, um die Variation sowohl der Respiration als auch des Priming-Effekts mit der Zusammensetzung der organischen Bodensubstanz zu erklären. Py-GC/MS-Daten wurden durch Hauptkomponentenanalyse (PCA) in mehrere lineare Achsen reduziert und die ersten drei Hauptkomponentenachsen (PC1, PC2, PC3) wurden stellvertretend für die Zusammensetzung der organischen Bodensubstanz als erklärende Variablen in den standardisierten LME Modellen verwendet.

Unsere Py-GC/MS-Daten deuten darauf hin, dass das organische Material mit zunehmender Bodentiefe verstärkt mikrobiell umgesetzt war. Die Abnahme der Qualität des organischen Materials wird auch durch den Rückgang von Kohlenhydraten und Ligninen bei gleichzeitiger Zunahme von aromatischen und phenolischen Verbindungen deutlich. Daraus schließen wir, dass die organische Bodensubstanz im Oberboden zu einem großen Teil aus pflanzlichem organischen Material bestand, während es im mineralischen Boden größtenteils aus mikrobiellen Verbindungen zusammengesetzt war.

Unser standardisiertes LME Modell der Respiration zeigte, dass in Oberböden die Respiration am höchsten war, wenn ein hoher Anteil an

Kohlenhydraten und Ligninen verfügbar war, während die Respiration in mineralischen Böden nicht durch die Veränderung der Zusammensetzung des organischen Materials beeinflusst wurde. Daraus schließen wir, dass die Qualität des organischen Materials nur in Oberbodenhorizonten, in denen stetig labile pflanzliche Verbindungen vorhanden waren, einen Einfluss auf die Mineralisierung hatte.

Unsere standardisierten LME-Modelle zeigten außerdem, dass die Zusammensetzung der organischen Bodensubstanzen das Ausmaß des Priming-Effekts beeinflusst. Diese Beziehung war jedoch abhängig von dem hinzugefügten Substrat. Wir stellten fest, dass die Zusammensetzung des organischen Materials die Variation des Priming-Effekts, verursacht durch die Zugabe von organischem Kohlenstoff (Cellulose) alleine, nicht erklären konnte. Das legt nahe, dass eine Linderung einer möglichen mikrobiellen Energielimitierung allein nicht eine Beziehung zwischen organischer Bodensubstanz und Respiration erklärt. Im Gegensatz dazu fanden wir bei Zugabe von organischem Stickstoff (Protein), dass der Priming-Effekt in Böden mit organischem Material von schlechter Qualität, die sich durch hohe Aromaten- und Phenolgehalte auszeichnen, am höchsten war. Die Zugabe eines kohlenstoff- und stickstoffhaltigen Substrats (Protein) könnte die mikrobiellen Anforderungen für ein Wachstum besser erfüllt haben. Außerdem könnte der zusätzliche Stickstoff in die Produktion von extrazellulären Enzymen investiert worden sein, was den Abbau der aromatischen und phenolischen Fraktion des organischen Materials ermöglicht, die vor der Substratzugabe aufgrund eines Mangels an extrazellulären Enzymen nicht zersetzt werden konnte.

Mit unserer Studie konnten wir zeigen, dass die Zusammensetzung des bodeneigenen organischen Materials sowohl die Respiration als auch die Größe des Priming-Effekts beeinflusst. Wir schlagen jedoch vor, dass organischer Stickstoff eine entscheidende Rolle spielt, damit dieser Zusammenhang sichtbar wird. Die Zusammensetzung des organischen Materials übt nur dann ihren Einfluss auf den Priming-Effekt aus, wenn Mikroben sowohl mit Kohlenstoff als auch mit Stickstoff versorgt werden.

PART 4

References

Allison, S. D., LeBauer, D. S., Ofrecio, M. R., Reyes, R., Ta, A.-M., & Tran, T. M. (2009). Low levels of nitrogen addition stimulate decomposition by boreal forest fungi. *Soil Biology and Biochemistry*, *41*, 293–302. https://doi.org/10.1016/J.SOILBIO.2008.10.032

AMAP. (2011). *Snow, Water, Ice and Permafrost in the Arctic (SWIPA): Climate Change and the Cryosphere*. Arctic Monitoring and Assessment Programme (AMAP), Oslo, Norway.

Bhatt, U. S., Walker, D. A., Raynolds, M. K., Comiso, J. C., Epstein, H. E., Jia, G., … Webber, P. J. (2010). Circumpolar Arctic tundra vegetation change is linked to sea ice decline. *Earth Interactions*, *14*(8). https://doi.org/10.1175/2010EI315.1

Bingeman, C. W., Varner, J. E., & Martin, W. P. (1953). The effect of the addition of organic materials on the decomposition of an organic soil. *Soil Science Society of America*, *29*, 692–696.

Blagodatskaya, E., Khomyakov, N., Myachina, O., Bogomolova, I., Blagodatsky, S., & Kuzyakov, Y. (2014). Microbial interactions affect sources of priming induced by cellulose. *Soil Biology and Biochemistry*, *74*, 39–49. https://doi.org/10.1016/j.soilbio.2014.02.017

Blagodatskaya, E., & Kuzyakov, Y. (2008). Mechanisms of real and apparent priming effects and their dependence on soil microbial biomass and community structure: Critical review. *Biology and Fertility of Soils*, *45*, 115–131. https://doi.org/10.1007/s00374-008-0334-y

Blagodatskaya, E. V, Blagodatsky, S. A., Anderson, T.-H., & Kuzyakov, Y. (2007). Priming effects in Chernozem induced by glucose and N in relation to microbial growth strategies. *Applied Soil Ecology*, *37*(1–2), 95–105. https://doi.org/10.1016/J.APSOIL.2007.05.002

Bockheim, J. G. (2007). Importance of Cryoturbation in Redistributing Organic Carbon in Permafrost-Affected Soils. *Soil Science Society of America Journal*, *71*, 1335–1342. https://doi.org/10.2136/sssaj2006.0414N

Brown, J., Ferrians, J. O. J., Heginbottom, J. A., & Melnikov, E. S. (1998). Circum-Arctic map of permafrost and ground-ice conditions.

Buurman, P., Van Bergen, P. F., Jongmans, A. G., Meijer, E. L., Duran, B., & Van Lagen, B. (2005). Spatial and temporal variation in podzol organic matter studied by pyrolysis-gas chromatography/mass spectrometry and micromorphology. *European Journal of Soil Science*, *56*, 253–270. https://doi.org/10.1111/j.1365-2389.2004.00662.x

Capek, P., Di Akov A, K. R., Dickopp, J.-E. E., Rí, J., Arta, B., Wild, B., … Šantrůčková, H. (2015). The effect of warming on the vulnerability of subducted organic carbon in arctic soils. *Soil Biology and Biochemistry*, *90*, 19–29. https://doi.org/10.1016/j.soilbio.2015.07.013

Carr, A. S., Boom, A., Chase, B. M., Roberts, D. L., & Roberts, Z. E. (2010). Molecular fingerprinting of wetland organic matter using pyrolysis-GC/MS: An example from the southern Cape coastline of South Africa. *Journal of Paleolimnology*, *44*, 947–961. https://doi.org/10.1007/s10933-010-9466-9

Chen, R., Senbayram, M., Blagodatsky, S., Myachina, O., Dittert, K., Lin, X., … Kuzyakov, Y. (2014). Soil C and N availability determine the priming effect: Microbial N mining and stoichiometric decomposition theories. *Global Change Biology*, *20*, 2356–2367. https://doi.org/10.1111/gcb.12475

Cheng, W., Parton, W. J., Gonzalez-Meler, M. A., Phillips, R., Asao, S., McNickle, G. G.,

… Jastrow, J. D. (2014). Synthesis and modeling perspectives of rhizosphere priming. *New Phytologist*. https://doi.org/10.1111/nph.12440
Craine, J. M., Morrow, C., & Fierer, N. (2007). MICROBIAL NITROGEN LIMITATION INCREASES DECOMPOSITION. *Ecology*, *88*(8), 2105–2113. https://doi.org/10.1890/06-1847.1
Dao, T. T., Gentsch, N., Mikutta, R., Sauheitl, L., Shibistova, O., Wild, B., … Guggenberger, G. (2018). Fate of carbohydrates and lignin in north-east Siberian permafrost soils. *Soil Biology and Biochemistry*, *116*, 311–322. https://doi.org/10.1016/j.soilbio.2017.10.032
Davidson, E. A., & Janssens, I. A. (2006). Temperature sensitivity of soil carbon decomposition and feedbacks to climate change. *Nature*, *440*(7081), 165–173. https://doi.org/10.1038/nature04514
De Nobili, M., Contin, M., Mondini, C., & Brookes, P. C. (2001). Soil microbial biomass is triggered into activity by trace amounts of substrate. *Soil Biology and Biochemistry*, *33*, 1163–1170. https://doi.org/10.1016/S0038-0717(01)00020-7
Di Lonardo, D. P., De Boer, W., Klein Gunnewiek, P. J. A., Hannula, S. E., & Van der Wal, A. (2017). Priming of soil organic matter: Chemical structure of added compounds is more important than the energy content. *Soil Biology and Biochemistry*, *108*, 41–54. https://doi.org/10.1016/j.soilbio.2017.01.017
Dijkstra, F. A., Carrillo, Y., Pendall, E., & Morgan, J. A. (2013). Rhizosphere priming: a nutrient perspective. *Frontiers in Microbiology*, *4*. https://doi.org/10.3389/fmicb.2013.00216
Don, A., Rödenbeck, C., & Gleixner, G. (2013). Unexpected control of soil carbon turnover by soil carbon concentration. *Environmental Chemistry Letters*, *11*, 407–413. https://doi.org/10.1007/s10311-013-0433-3
Drake, J. E., Darby, B. A., Giasson, M. A., Kramer, M. A., Phillips, R. P., & Finzi, A. C. (2013). Stoichiometry constrains microbial response to root exudation-insights from a model and a field experiment in a temperate forest. *Biogeosciences*, *10*, 821–838. https://doi.org/10.5194/bg-10-821-2013
Drake, T. W., Wickland, K. P., Spencer, R. G. M., McKnight, D. M., & Striegl, R. G. (2015). Ancient low–molecular-weight organic acids in permafrost fuel rapid carbon dioxide production upon thaw. *Proceedings of the National Academy of Sciences*, *112*(45), 13946–13951. https://doi.org/10.1073/pnas.1511705112
Dutta, K., Schuur, E. A. G., Neff, J. C., & Zimov, S. A. (2006). Potential carbon release from permafrost soils of Northeastern Siberia. *Global Change Biology*, *12*, 2336–2351. https://doi.org/10.1111/j.1365-2486.2006.01259.x
Euskirchen, E. S., McGuire, A. D., Kicklighter, D. W., Zhuang, Q., Clein, J. S., Dargaville, R. J., … Smith, N. V. (2006). Importance of recent shifts in soil thermal dynamics on growing season length, productivity, and carbon sequestration in terrestrial high-latitude ecosystems. *Global Change Biology*, *12*, 731–750. https://doi.org/10.1111/j.1365-2486.2006.01113.x
Fontaine, S., Barot, S., Barré, P., Bdioui, N., Mary, B., & Rumpel, C. (2007). Stability of organic carbon in deep soil layers controlled by fresh carbon supply. *Nature*, *450*, 277–280. https://doi.org/10.1038/nature06275
Fontaine, S., Henault, C., Aamor, A., Bdioui, N., Bloor, J. M. G., Maire, V., … Maron, P. A. (2011). Fungi mediate long term sequestration of carbon and nitrogen in soil through their priming effect. *Soil Biology and Biochemistry*, *43*, 86–96. https://doi.org/10.1016/j.soilbio.2010.09.017
Fontaine, S., Mariotti, A., & Abbadie, L. (2003). The priming effect of organic matter: a question of microbial competition? *Soil Biology & Biochemistry*, *35*, 837–843. https://doi.org/10.1016/S0038-0717(03)00123-8
Garcia-Pausas, J., & Paterson, E. (2011). Microbial community abundance and structure are determinants of soil organic matter mineralisation in the presence of labile carbon. *Soil Biology and Biochemistry*, *43*, 1705–1713. https://doi.org/10.1016/j.soilbio.2011.04.016

Gelman, A., & Su, Y.-S. (2015). arm: Data Analysis Using Regression and Multilevel/Hierarchical Models. R package version 1.8-6. Retrieved from http://cran.r-project.org/package=arm

Gentsch, N., Mikutta, R., Alves, R. J. E., Barta, J., Čapek, P., Gittel, A., … Šantruˇčková, H. (2015). Storage and transformation of organic matter fractions in cryoturbated permafrost soils across the Siberian Arctic. *Biogeosciences*, *12*, 4525–4542. https://doi.org/10.5194/bg-12-4525-2015

Grosse, G., Goetz, S., McGuire, A. D., Romanovsky, V. E., & Schuur, E. A. G. (2016). Changing permafrost in a warming world and feedbacks to the Earth system. *Environmental Research Letters*, *11*(4). https://doi.org/10.1088/1748-9326/11/4/040201

Grosse, G., Harden, J. W., Turetsky, M. R., McGuire, A. D., Camill, P., Tarnocai, C., … Striegl, R. G. (2011). Vulnerability of high-latitude soil organic carbon in North America to disturbance. *Journal of Geophysical Research: Biogeosciences*, *116*(3), 1–23. https://doi.org/10.1029/2010JG001507

Grosse, G., Romanovsky, V. E., Jorgenson, T., Anthony, K. W., Brown, J., & Overduin, P. P. (2011). Vulnerability and Feedbacks of Permafrost to Climate Change. *EOS, Transsactions, American Geophysical Union*, *92*(9), 73–80. https://doi.org/10.1029/2011EO090001.

Guenet, B., Neill, C., Bardoux, G., & Abbadie, L. (2010). Is there a linear relationship between priming effect intensity and the amount of organic matter input? *Applied Soil Ecology*, *46*(3), 436–442. https://doi.org/10.1016/J.APSOIL.2010.09.006

Hamer, U., & Marschner, B. (2005). Priming effects in different soil types induced by fructose, alanine, oxalic acid and catechol additions. *Soil Biology and Biochemistry*, *37*(3), 445–454. https://doi.org/10.1016/j.soilbio.2004.07.037

Hartley, I. P., Garnett, M. H., Sommerkorn, M., Hopkins, D. W., Fletcher, B. J., Sloan, V. L., … Wookey, P. A. (2012). A potential loss of carbon associated with greater plant growth in the European Arctic. *Nature Climate Change*, *2*(12), 875–879. https://doi.org/10.1038/nclimate1575

Heimann, M., & Reichstein, M. (2008). Terrestrial ecosystem carbon dynamics and climate feedbacks. *Nature*, *451*, 289–292. https://doi.org/10.1038/nature06591

Helsel, D. R. (2012). *Statistics for censored environmental data using Minitab and R* (2nd ed.). Hoboken, New Jersey: John Wiley & Sons, Inc.

Hernández, D. L., & Hobbie, S. E. (2010). The effects of substrate composition, quantity, and diversity on microbial activity. *Plant and Soil*, *335*, 397–411. https://doi.org/10.1007/s11104-010-0428-9

Hicks Pries, C. E., Schuur, E. A. G., Natali, S. M., & Crummer, K. G. (2016). Old soil carbon losses increase with ecosystem respiration in experimentally thawed tundra. *Nature Climate Change*, *6*(2), 214–218. https://doi.org/10.1038/nclimate2830

Hugelius, G., Bockheim, J. G., Camill, P., Elberling, B., Grosse, G., Harden, J. W., … Yu, Z. (2013). A new data set for estimating organic carbon storage to 3 m depth in soils of the northern circumpolar permafrost region. *Earth System Science Data*, *5*, 393–402. https://doi.org/10.5194/essd-5-393-2013

Hugelius, G., Strauss, J., Zubrzycki, S., Harden, J. W., Schuur, E. A. G., Ping, C.-L., … Kuhry, P. (2014). Estimated stocks of circumpolar permafrost carbon with quantified uncertainty ranges and identified data gaps. *Biogeosciences*, *11*, 6573–6593. https://doi.org/10.5194/bg-11-6573-2014

IPCC. (2013). *Climate Change 2013: The Physical Science Basis. Contribution of Working Group I to the Fifth Assessment Report of the Intergovernmental Panel on Climate Change*. [Stocker, T.F., D. Qin, G.-K. Plattner, M. Tignor, S.K. Allen, J. Boschung, A. Nauels, Y. Xia, V. Bex and P.M. Midgley(eds.)] Cambridge University Press, Cambridge, United Kingdom and New York, NY, USA. https://doi.org/10.1017/CBO9781107415324

IPCC. (2014). *Climate Change 2014: Synthesis Report. Contribution of Working Groups I, II and III to the Fifth Assessment Report of the Intergovernmental Panel on*

Climate Change. [Core Writing Team, R.K. Pachauri and L.A. Meyer (eds.)]. IPCC, Geneva, Schwitzerland: IPCC.
Jagadamma, S., Mayes, M. A., Steinweg, J. M., & Schaeffer, S. M. (2014). Substrate quality alters the microbial mineralization of added substrate and soil organic carbon. *Biogeosciences*, *11*(17), 4665–4678. https://doi.org/10.5194/bg-11-4665-2014
Jenkinson, D. S., Fox, R. H., & Rayner, J. H. (1985). Interactions between fertilizer nitrogen and soil nitrogen—the so-called "priming" effect. *European Journal of Soil Science*, *36*(3), 425–444.
Jones, D. L., Nguyen, C., & Finlay, R. D. (2009). Carbon flow in the rhizosphere: Carbon trading at the soil-root interface. *Plant and Soil*, *321*, 5–33. https://doi.org/10.1007/s11104-009-9925-0
Kaal, J., Baldock, J. A., Buurman, P., Nierop, K. G. J., Pontevedra-Pombal, X., & Martínez-Cortizas, A. (2007). Evaluating pyrolysis–GC/MS and 13C CPMAS NMR in conjunction with a molecular mixing model of the Penido Vello peat deposit, NW Spain. *Organic Geochemistry*, *38*(7), 1097–1111. https://doi.org/10.1016/J.ORGGEOCHEM.2007.02.008
Khvorostyanov, D. V., Krinner, G., Ciais, P., Heimann, M., & Zimov, S. A. (2008). Vulnerability of permafrost carbon to global warming. Part I: Model description and role of heat generated by organic matter decomposition. *Tellus B: Chemical and Physical Meteorology*, *60:2*, 250–264. https://doi.org/10.1111/j.1600-0889.2007.00333.x
Koven, C. D., Ringeval, B., Friedlingstein, P., Ciais, P., Cadule, P., Khvorostyanov, D. V., … Tarnocai, C. (2011). Permafrost carbon-climate feedbacks accelerate global warming. *Proceedings of the National Academy of Sciences*, *108*(36), 14769–14774. https://doi.org/10.1073/pnas.1103910108
Kuzyakov, Y. (2010). Priming effects: Interactions between living and dead organic matter. *Soil Biology and Biochemistry*, *42*, 1363–1371. https://doi.org/10.1016/j.soilbio.2010.04.003
Kuzyakov, Y., Friedel, J. K., & Stahr, K. (2000). Review of mechanisms and quantification of priming effects. *Soil Biology & Biochemistry*, *32*, 1485–1498. https://doi.org/10.1016/S0038-0717(00)00084-5
Lawrence, D. M., Slater, A. G., & Swenson, S. C. (2012). Simulation of present-day and future permafrost and seasonally frozen ground conditions in CCSM4. *Journal of Climate*, *25*(7), 2207–2225. https://doi.org/10.1175/JCLI-D-11-00334.1
Le Cao, K.-A., Gonzalez, I., Dejean, S. with key contributors, Rohart, F., Gautier, B., contriubtions from Monget, P., … Liquet, B. (2015). mixOmics: Omics Data Integration Project. R package version 5.2.0.
Lisitsyna, O. M., & Romanovskii, N. N. (1998). Dynamics of permafrost in Northern Eurasia during the last 20,000 years. In *Proceedings of the Seventh International Permafrost Conference* (pp. 675–681). Yellowknife, Canada, June 23-27.
Liu, X.-J. A., Sun, J., Mau, R. L., Finley, B. K., Compson, Z. G., van Gestel, N., … Hungate, B. A. (2017). Labile carbon input determines the direction and magnitude of the priming effect. *Applied Soil Ecology*, *109*, 7–13. https://doi.org/10.1016/j.apsoil.2016.10.002
Ma, X.-M., Lu, R., & Miyakoshi, T. (2014). Application of Pyrolysis Gas Chromatography/Mass Spectrometry in Lacquer Research: A Review. *Polymers*, *6*(1), 132–144. https://doi.org/10.3390/polym6010132
Mikutta, R., Kleber, M., Torn, M. S., & Jahn, R. (2006). Stabilization of soil organic matter: Association with minerals or chemical recalcitrance? *Biogeochemistry*, *77*, 25–56. https://doi.org/10.1007/s10533-005-0712-6
Natali, S. M., Schuur, E. A. G., & Rubin, R. L. (2012). Increased plant productivity in Alaskan tundra as a result of experimental warming of soil and permafrost. *Journal of Ecology*, *100*, 488–498. https://doi.org/10.1111/j.1365-2745.2011.01925.x
Nierop, K. G. J., Pulleman, M. M., & Marinissen, J. C. Y. (2001). Management induced

organic matter differentiation in grassland and arable soil: a study using pyrolysis techniques. *Soil Biology and Biochemistry*, *33*(6), 755–764. https://doi.org/10.1016/S0038-0717(00)00223-6

Nikrad, M. P., Kerkhof, L. J., & Häggblom, M. M. (2016). The subzero microbiome: Microbial activity in frozen and thawing soils. *FEMS Microbiology Ecology*, *92*, 1–16. https://doi.org/10.1093/femsec/fiw081

Ninnes, S., Tolu, J., Meyer-Jacob, C., Mighall, T. M., & Bindler, R. (2017). Investigating molecular changes in organic matter composition in two Holocene lake-sediment records from central Sweden using pyrolysis-GC/MS. *Journal of Geophysical Research: Biogeosciences*, *122*(6), 1423–1438. https://doi.org/10.1002/2016JG003715

Paré, M. C., & Bedard-Haughn, A. (2013). Soil organic matter quality influences mineralization and GHG emissions in cryosols: A field-based study of sub- to high Arctic. *Global Change Biology*, *19*(4), 1126–1140. https://doi.org/10.1111/gcb.12125

Ping, C. L., Bockheim, J. G., Kimble, J. M., Michaelson, G. J., & Walker, D. A. (1998). Characteristics of cryogenic soils along a latitudinal transect in arctic Alaska. *Journal of Geophysical Research*, *103*, 28917– 28928.

Pinheiro, J., Bates, D., DebRoy, S., Sarkar, D., & R Core Team. (2015). _nlme: Linear and Nonlinear Mixed Effects Models_. R package version 3.1-120. Retrieved from http://cran.r-project.org/package=nlme

R Development Core Team. (2015). *R: A language and environment for statistical computing*. R Foundation for Statistical Computing, Vienna, Austria. Retrieved from http://www.r-project.org.

Richter-Menge, J., Overland, J. E., Mathis, J. T., Osborne, E., & Eds. (2017). *Arctic Report Card 2017*. *http://www.arctic.noaa.gov/Report-Card*.

Romanovsky, V. E., Drozdov, D. S., Oberman, N. G., Malkova, G. V, Kholodov, A. L., Marchenko, S. S., … Vasiliev, A. A. (2010). Thermal state of permafrost in Russia. *Permafrost and Periglacial Processes*, *21*(2), 136–155. https://doi.org/10.1002/ppp.683

Romanovsky, V. E., Garagula, L. S., & Seregina, N. V. (1992). Freezing and thawing of soils under the influence of 300- and 90-year periods of temperature fluctuation. In *Proceedings of the International Conference on the Role of Polar Regions in Global Change* (pp. 543–548). University of Alaska Fairbanks.

Romanovsky, V. E., Kholodov, A. L., Marchenko, S. S., Oberman, N. G., Drozdov, D. S., Malkova, G. V, … Zheleznyak, M. N. (2008). Thermal State and Fate of Permafrost in Russia: First Results of IPY, *29*, 1511–1518.

Romanovsky, V. E., Smith, S. L., & Christiansen, H. H. (2010). Permafrost thermal state in the polar northern hemisphere during the international polar year 2007-2009: A synthesis. *Permafrost and Periglacial Processes*, *21*, 106–116. https://doi.org/10.1002/ppp.689

Ruiz-Dueñas, F. J., & Martínez, Á. T. (2009). Microbial degradation of lignin: How a bulky recalcitrant polymer is efficiently recycled in nature and how we can take advantage of this. *Microbial Biotechnology*, *2*(2 SPEC. ISS.), 164–177. https://doi.org/10.1111/j.1751-7915.2008.00078.x

Rumpel, C., Eusterhues, K., & Kögel-Knabner, I. (2004). Location and chemical composition of stabilized organic carbon in topsoil and subsoil horizons of two acid forest soils. *Soil Biology and Biochemistry*, *36*(1), 177–190. https://doi.org/10.1016/j.soilbio.2003.09.005

Rumpel, C., & Kögel-Knabner, I. (2011). Deep soil organic matter-a key but poorly understood component of terrestrial C cycle. *Plant and Soil*, *338*, 143–158. https://doi.org/10.1007/s11104-010-0391-5

Saito, K., Kimoto, M., Zhang, T., Takata, K., & Emori, S. (2007). Evaluating a high-resolution climate model: Simulated hydrothermal regimes in frozen ground regions and their change under the global warming scenario. *Journal of Geophysical Research: Earth Surface*, *112*(2), 1–19. https://doi.org/10.1029/2006JF000577

Schellekens, J., Buurman, P., & Pontevedra-Pombal, X. (2009). Selecting parameters for the environmental interpretation of peat molecular chemistry – A pyrolysis-GC/MS study. *Organic Geochemistry*, *40*(6), 678–691. https://doi.org/10.1016/J.ORGGEOCHEM.2009.03.006

Schimel, J. P., & Weintraub, M. N. (2003). The implications of exoenzyme activity on microbial carbon and nitrogen limitation in soil: a theoretical model. *Soil Biology and Biochemistry*, *35*(4), 549–563. https://doi.org/10.1016/S0038-0717(03)00015-4

Schirrmeister, L., Grosse, G., Wetterich, S., Overduin, P. P., Strauss, J., Schuur, E. A. G., & Hubberten, H.-W. (2011). Fossil organic matter characteristics in permafrost deposits of the northeast Siberian Arctic. *Journal of Geophysical Research: Biogeosciences*, *116*, G00M02. https://doi.org/10.1029/2011JG001647

Schirrmeister, L., Siegert, C., Kuznetsova, T., Kuzmina, S., Andreev, A., Kienast, F., … Bobrov, A. (2002). Paleoenvironmental and paleoclimatic records from permafrost deposits in the Arctic region of Northern Siberia. *Quaternary International*, *89*(1), 97–118. https://doi.org/10.1016/S1040-6182(01)00083-0

Schmidt, M. W. I. I., Torn, M. S., Abiven, S., Dittmar, T., Guggenberger, G., Janssens, I. A., … Ko, I. (2011). Persistence of soil organic matter as an ecosystem property. *Nature*, *478*, 49–56. https://doi.org/10.1038/nature10386

Schnecker, J., Wild, B., Hofhansl, F., Alves, R. J. E., Bárta, J., Apek, P. Č., … Richter, A. (2014). Effects of Soil Organic Matter Properties and Microbial Community Composition on Enzyme Activities in Cryoturbated Arctic Soils. *PLoS ONE*, *9*(4). https://doi.org/10.1371/journal.pone.0094076

Schnecker, J., Wild, B., Takriti, M., Alves, R. J. E., Gentsch, N., Gittel, A., … Richter, A. (2015). Microbial community composition shapes enzyme patterns in topsoil and subsoil horizons along a latitudinal transect in Western Siberia. *Soil Biology & Biochemistry*, *83*, 106–115.

Schuur, E. A. G., Abbott, B. W., Bowden, W. B., Brovkin, V., Camill, P., Canadell, J. G., … Zimov, S. A. (2013). Expert assessment of vulnerability of permafrost carbon to climate change. *Climatic Change*, *119*, 359–374. https://doi.org/10.1007/s10584-013-0730-7

Schuur, E. A. G., Bockheim, J., Canadell, J. G., Euskirchen, E., Field, C. B., Goryachkin, S. V, … Zimov, S. A. (2008). Vulnerability of permafrost carbon to climate change: Implications for the global carbon cycle. *BioScience*, *58*(8), 701–714. https://doi.org/10.1641/B580807

Schuur, E. A. G., McGuire, A. D., Schädel, C., Grosse, G., Harden, J. W., Hayes, D. J., … Vonk, J. E. (2015). Climate change and the permafrost carbon feedback. *Nature*, *520*, 171–179. https://doi.org/10.1038/nature14338

Seo, J. S., Keum, Y. S., & Li, Q. X. (2009). *Bacterial degradation of aromatic compounds*. *International Journal of Environmental Research and Public Health* (Vol. 6). https://doi.org/10.3390/ijerph6010278

Sinsabaugh, R. L. (2010). Phenol oxidase, peroxidase and organic matter dynamics of soil. *Soil Biology and Biochemistry*, *42*(3), 391–404. https://doi.org/10.1016/J.SOILBIO.2009.10.014

Sistla, S. A., Moore, J. C., Simpson, R. T., Gough, L., Shaver, G. R., & Schimel, J. P. (2013). Long-term warming restructures Arctic tundra without changing net soil carbon storage. *Nature*, *497*(7451), 615–617. https://doi.org/10.1038/nature12129

Spohn, M., Klaus, K., Wanek, W., & Richter, A. (2016). Microbial carbon use efficiency and biomass turnover times depending on soil depth - Implications for carbon cycling. *Soil Biology and Biochemistry*, (96), 74–81. https://doi.org/10.1016/j.soilbio.2016.01.016

Stewart, C. E. (2012). Evaluation of angiosperm and fern contributions to soil organic matter using two methods of pyrolysis-gas chromatography-mass spectrometry. *Plant and Soil*, *351*, 31–46. https://doi.org/10.1007/s11104-011-0927-3

Van der Wal, A., & De Boer, W. (2017). Dinner in the dark: Illuminating drivers of soil organic matter decomposition. *Soil Biology and Biochemistry*, *105*, 45–48.

https://doi.org/10.1016/j.soilbio.2016.11.006
Van Everdingen, R. O. (ed. . (1998). *Multi-language Glossary of Permafrost and Related Ground-Ice Terms*.
Vancampenhout, K., Wouters, K., De Vos, B., Buurman, P., Swennen, R., & Deckers, J. (2009). Differences in chemical composition of soil organic matter in natural ecosystems from different climatic regions - A pyrolysis-GC/MS study. *Soil Biology and Biochemistry*, *41*, 568–579. https://doi.org/10.1016/j.soilbio.2008.12.023
Vance, E. . D., Chapin, F. S., & Chapin III, F. . (2001). Substrate limitations to microbial activity in taiga forest floors. *Soil Biology and Biochemistry*, *33*(2), 173–188. https://doi.org/10.1016/S0038-0717(00)00127-9
Velichko, A. A., & Faustova, M. A. (2009). Glaciation during the Late Pleistocene. In *Velichko, A.A. (Ed.). Paleoclimates and paleoenvironments of extra-tropical area of the Northern Hemisphere. Late Pleistocene - Holocene* (pp. 32–42). GEOS, Moscow.
Velichko, A. A., & Nechaev, V. P. (2005). *Cenozoic climatic and environmental changes in Russia*. edited by H.E. Wright jr., T.A. Blyakharchuk, A.A. Velichko & O. Borisova. Special Paper 382. The Geological Society of America.
Velichko, A. A., & Nechaev, V. P. (2009). Subaerial cryolithozone of the Northern Hemisphere during the Late Pleistocene and Holocene. In *Velichko, A.A. (Ed.). Paleoclimates and Paleoenvironments of Extra-tropical area of the Northern Hemisphere. Late Pleistocene - Holocene* (pp. 42–49). GEOS, Moscow.
White, D. M., Garland, D. S., Beyer, L., & Yoshikawa, K. (2004). Pyrolysis-GC/MS fingerprinting of environmental samples. *Journal of Analytical and Applied Pyrolysis*, *71*, 107–118. https://doi.org/10.1016/S0165-2370(03)00101-3
Wickham, H. (2009). *ggplot2: Elegant Graphics for Data Analysis*. Springer-Verlag New York.
Wild, B., Gentsch, N., Čapek, P., Diáková, K., Alves, R. J. E., Bárta, J., … Richter, A. (2016). Plant-derived compounds stimulate the decomposition of organic matter in arctic permafrost soils. *Scientific Reports*, *6*(25607). https://doi.org/10.1038/srep25607
Wild, B., Schnecker, J., Alves, R. J. E., Barsukov, P., Bárta, J., Čapek, P., … Richter, A. (2014). Input of easily available organic C and N stimulates microbial decomposition of soil organic matter in arctic permafrost soil. *Soil Biology and Biochemistry*. https://doi.org/10.1016/j.soilbio.2014.04.014
Wild, B., Schnecker, J., Knoltsch, A., Takriti, M., Mooshammer, M., Gentsch, N., … Richter, A. (2015). Microbial nitrogen dynamics in organic and mineral soil horizons along a latitudinal transect in western Siberia. *Global Biogeochemical Cycles*, *29*, 567–582. https://doi.org/10.1002/2015GB005084.Received
Yang, Z., Wullschleger, S. D., Liang, L., Graham, D. E., & Gu, B. (2016). Effects of warming on the degradation and production of low-molecular-weight labile organic carbon in an Arctic tundra soil. *Soil Biology and Biochemistry*, *95*, 202–212. https://doi.org/10.1016/j.soilbio.2015.12.022
Yassir, I., & Buurman, P. (2012). Soil organic matter chemistry changes upon secondary succession in Imperata Grasslands, Indonesia: A pyrolysis–GC/MS study. *Geoderma*, *173–174*, 94–103. https://doi.org/10.1016/J.GEODERMA.2011.12.024
Yershov, E. (1998). *General Geocryology*. Cambridge: Cambridge University Press.
Zhu, B., Gutknecht, J. L. M., Herman, D. J., Keck, D. C., Firestone, M. K., & Cheng, W. (2014). Rhizosphere priming effects on soil carbon and nitrogen mineralization. *Soil Biology and Biochemistry*, *76*, 183–192. https://doi.org/10.1016/j.soilbio.2014.04.033
Zimov, S. A., Davydov, S. P., Zimova, G. M., Davydova, A. I., Schuur, E. A. G., Dutta, K., & Chapin III, F. S. (2006). Permafrost carbon: Stock and decomposability of a globally significant carbon pool. *Geophysical Research Letters*, *33*, L20502. https://doi.org/10.1029/2006GL027484